Summer 2019

Using the ERT method to differentiate resistivity anomalies attributed to natural and man-made activities

Ibrahim Faisal Alshareef

Department:

USING THE ERT METHOD TO DIFFERENTIATE RESISTIVITY ANOMALIES ATTRIBUTED TO NATURAL AND MAN-MADE ACTIVITIES

by

IBRAHIM FAISAL ALSHAREEF

A THESIS

Presented to the Faculty of the Graduate School of the

MISSOURI UNIVERSITY OF SCIENCE AND TECHNOLOGY

In Partial Fulfillment of the Requirements for the Degree

MASTER OF SCIENCE IN GEOLOGICAL ENGINEERING

2019

Approved by

Neil Anderson, Advisor
J. David Rogers
Evgeniy Torgashov

ABSTRACT

Karst terrain is considered to be a very complex topography compared with most other geological environments. Many features can be observed such as sinkholes, air-filled cavities, losing streams, and solution widened joints. These karst features can cause subsidence and damage infrastructure such as buildings and roads thus causing economic hardship and disruption of life. The typical geological and hydrological studies are not enough to understand the karst processes.

For this reason, two geophysical methods were involved in investigating the subsurface in the study area. In this research, the electrical resistivity tomography (ERT) and multichannel analysis of surface wave (MASW) data were acquired in Greene County southwest Missouri. The ERT is a geophysical method that more frequently used to map variations in lithology and moisture content in complex subsurface areas such as karst. MASW data were used to constrain to ERT interpretations, particularly the depth to bedrock.

The study aims were to use ERT and MASW to map the variable depth of the top bedrock, differentiate the anomaly zones of resistivity that can be caused naturally or by man-made, mapping variations in rock quality, mapping joint sets, and identifying possible. According to the interpretation of the ERT data, it is concluded that anomalies zones were attributed to the seepage of moisture content through the natural and man-made drainage pathways and the area that contain prominent joint sets.

ACKNOWLEDGMENTS

I would like to thank my advisor Dr. Neil Anderson for guiding and helping me throughout my study. Also I want to thank Dr. J. David Rogers and Dr. Evgeniy Torgashov who are members of my thesis committee. My thanks go to my family and friends. Finally, I would like to thank my writing editor Kelsi Leverett.

TABLE OF CONTENTS

LIST OF ILLUSTRATIONS

Page

LIST OF TABLES

Page

1. INTRODUCTION

In Missouri, 59% of the landscape is underlain by thick, carbonate rock units that contain complex karst topography. Karst topography is characterized by sinkholes, caves, air-filled cavities, losing streams, and solution widened joints. These features dominate the subsurface and create significant hazards to infrastructures such as buildings and roads. Subsidence and sinkhole collapse cost an estimated $300,000,000 per year in the United States; however, typical geological and hydrological studies are not enough to understand these complex karst processes. Unlike other natural hazards, sinkhole collapse, widening joints, and subsidence are not purely weather dependent and can occur sporadically as a result of the introduction of man-made structures in the subsurface. As more man-made infrastructure expands in to formerly rural karst terrain, more effective methods of investigating karst subsurface failures are needed.

In this research, two geophysical methods, electrical resistivity tomography (ERT) and multichannel analysis surface wave (MASW), were used to investigate the karst terrain in Greene County, Missouri. ERT data were used to map variations in the elevation of top of bedrock, soil thickness, and rock quality; identify joint sets; characterize existing sinkholes; and provide insight into groundwater flow patterns to a depth of approximately 100 feet. MASW data were acquired to a depth of approximately 50 ft to map variations in the depth to top of rock and soil thickness; determine the engineering properties of rock and soil; and to constrain ERT interpretations (particularly depth to bedrock).

The objectives of this study are to assess the efficacy of correlating ERT and MASW methodologies to:

1. Investigate whether variations in soil and bedrock moisture content detected using ERT can be correlated to surface topography
2. Differentiate between resistivity anomalies attributed to natural or man-made activities
3. Identify karst features such as sinkhole and air-filled cavities
4. Map the variable depth of the top bedrock and variations in rock quality

2. STUDY AREA

The study area is located in Greene County in southwestern Missouri (Figures 2.1and 2.2). Most of the landmass in the southwestern area of Missouri consists of low rounded hills that are dotted with springs, streams, and a range of karst features, like sinkholes, caves, springs. This is especially the case in the region in which the Springfield Plateau aquifer is located (Waite et al., 1993). The soil found in the study site is largely residuum. It is reasonably well drained with the land following a low slope (Waite et al., 1993).

According to Fellows (1970), the residual soil in the area takes the form of reddish-brown clay that contains admixed cherty fragments. The complex system of belowground cavities and caves could stimulate the differential settlement of the layers above, leading to the development of further sinkholes that form in the caverns. According to existing investigations that have focused on collating data on the geology of the region, from the bedrock down to the depth, the interrelated issues associated with the expanded area of joints could potentially have a detrimental impact on the stability of the project area. Boreholes have been drilled into the bedrock in the study site, and investigation of the extracts has revealed that the area consists of highly-dissolved Burlington-Keokuk Limestone, which is illustrated by the existence of cutters, pinnacles, and cavities (Fellows, 1970). In addition, there are variations in the bedrock depth, which entails that there is a lateral variation in the karst features that can be observed.

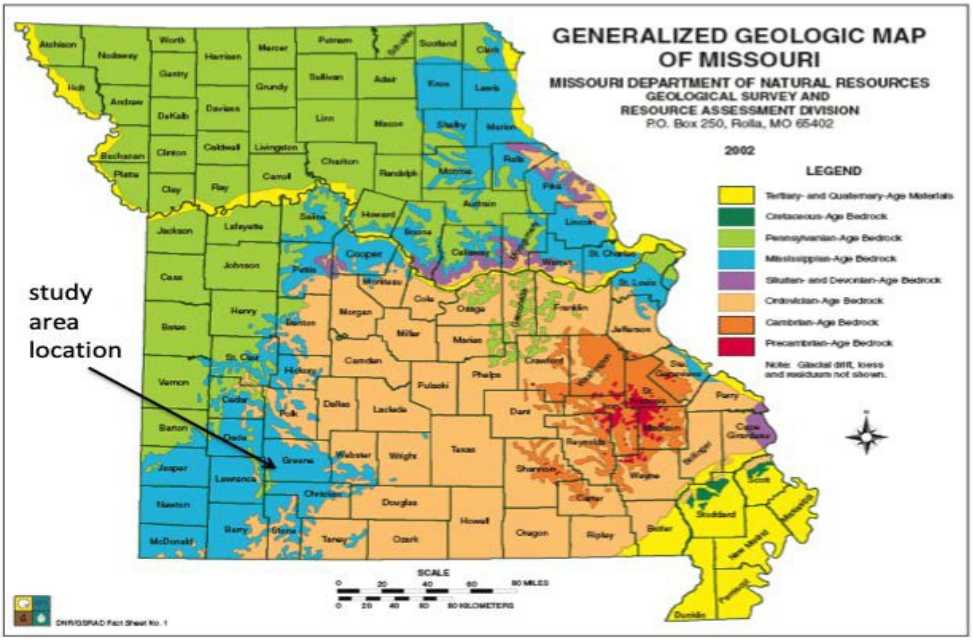

Figure 2.1. Shows the approximate location of the study area.

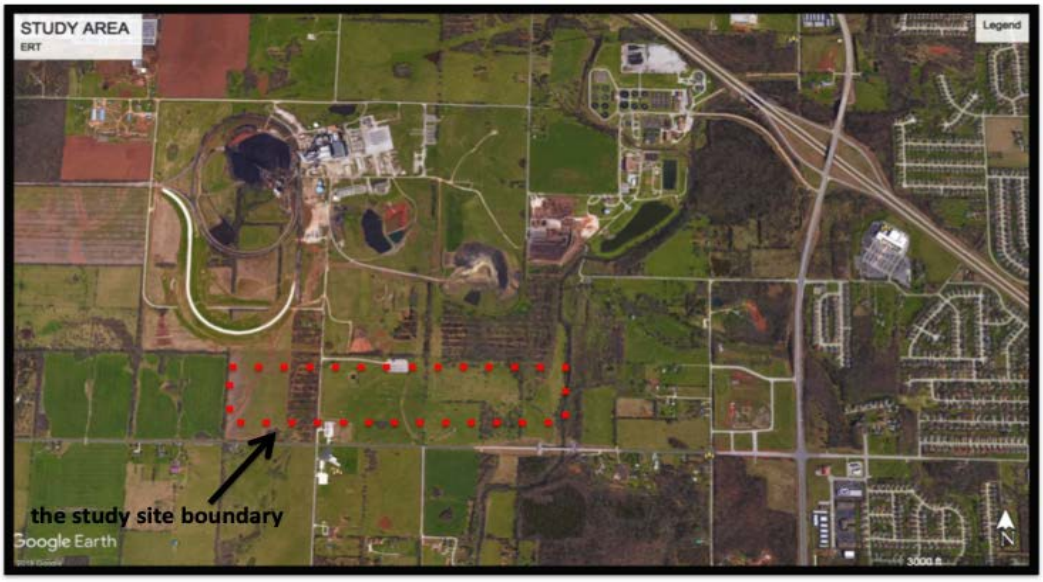

Figure 2.2. Represents the study site boundary.

3. GEOLOGICAL AND STRATIGRAPHIC SETTING

3.1 REGIONAL GEOLOGICAL SETTING

The Ozark Plateaus extends through four states: Missouri, Arkansas, Oklahoma, and Kansas. The plateaus cover approximately 60 percent of Missouri and are divided to three sections: Salem Plateau, Springfield Plateau, and Boston Mountain (Figure 3.1). Greene County is found in southwestern area of Missouri that is located in the Springfield Plateau. This plateau is underlain by the Burlington- Keokuk Limestone, bedrock of thick Mississippian-age limestones and cherty limestones that overlie Ordovician- and Cambrian-aged strata (Figure 3.2). The bedrock has significant faulting and folding and an irregular, extensively weathered bedrock surface covered with cherty clay residuum varying from a few feet to over 40 ft.

The fault systems in the Springfield Plateau are prominent aspects in this plateau. The majority of faults that are observed in Missouri typically trend in the northwest direction; however, a small number trend in the northeast direction (McCracken, 1966). The Seneca fault system found in the southwestern area of the plateau trend NW (Figure 3.3). According to McCracken (1971), the faults observed in Greene County trend NE and NW with high-angle gravity faults that have a vertical component up to 300 ft. These fault features have a direct influence on the drainage pattern in the Springfield Plateau particularly along the areas of fractured rocks known to trigger the karst processes.

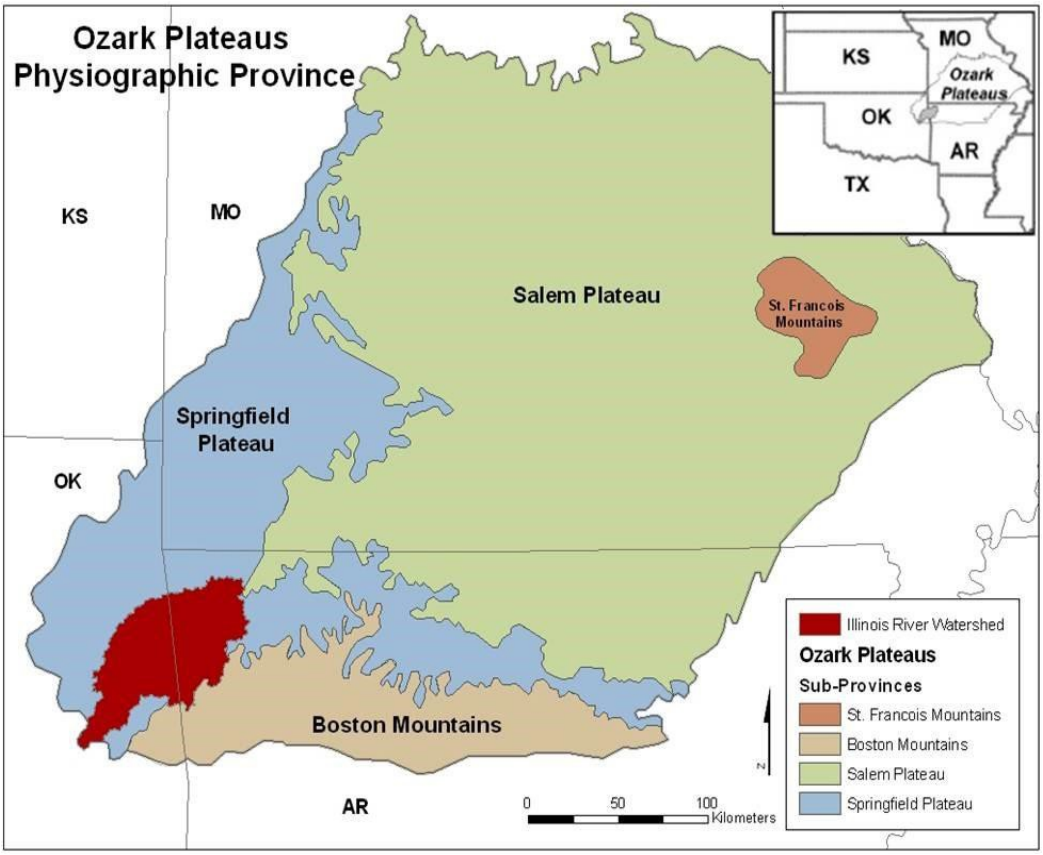

Figure 3.1. Shows the divisions of Ozark Plateaus.

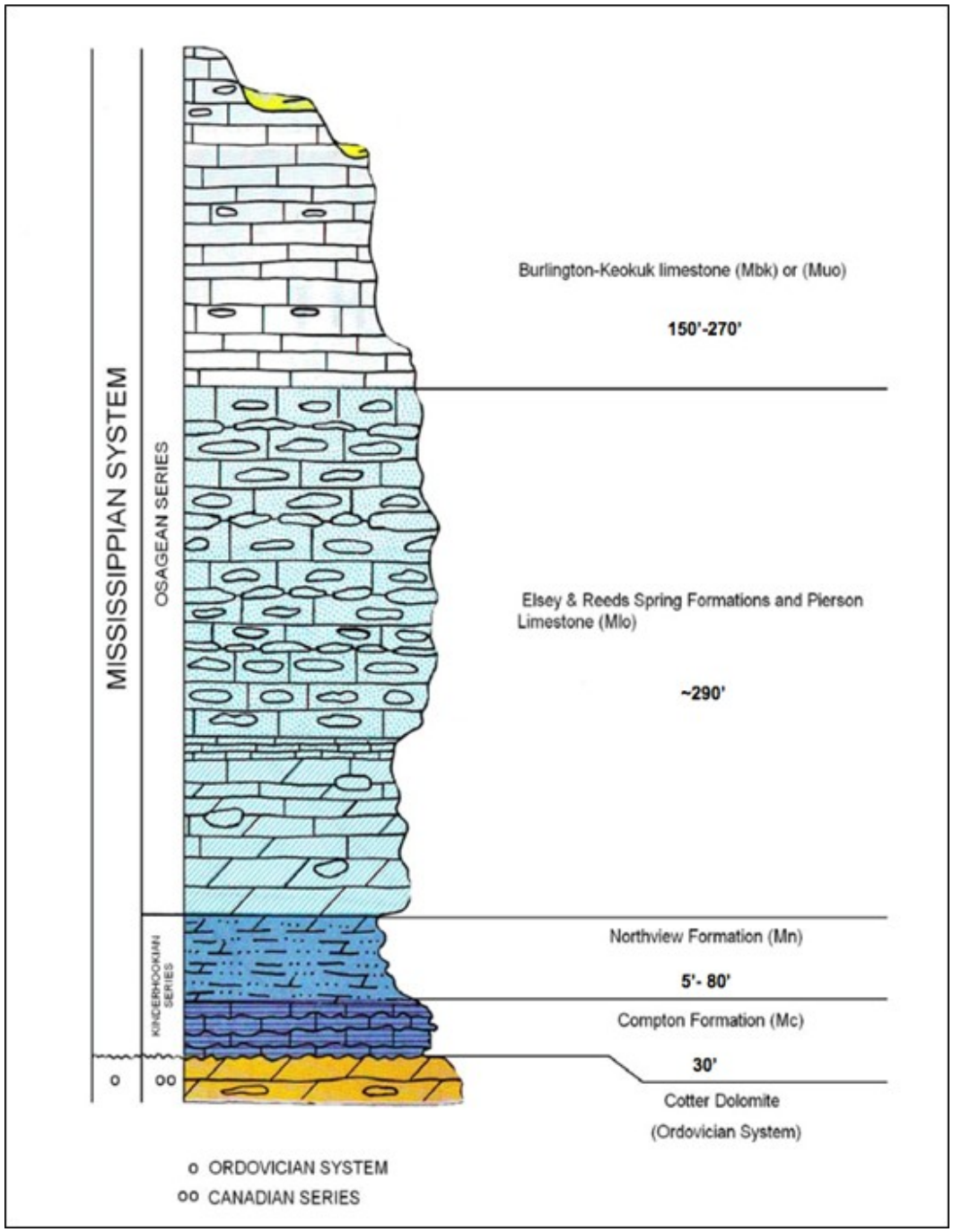

Figure 3.2. The geologic setting of the Mississippian system in the study area (Fellows, 1970).

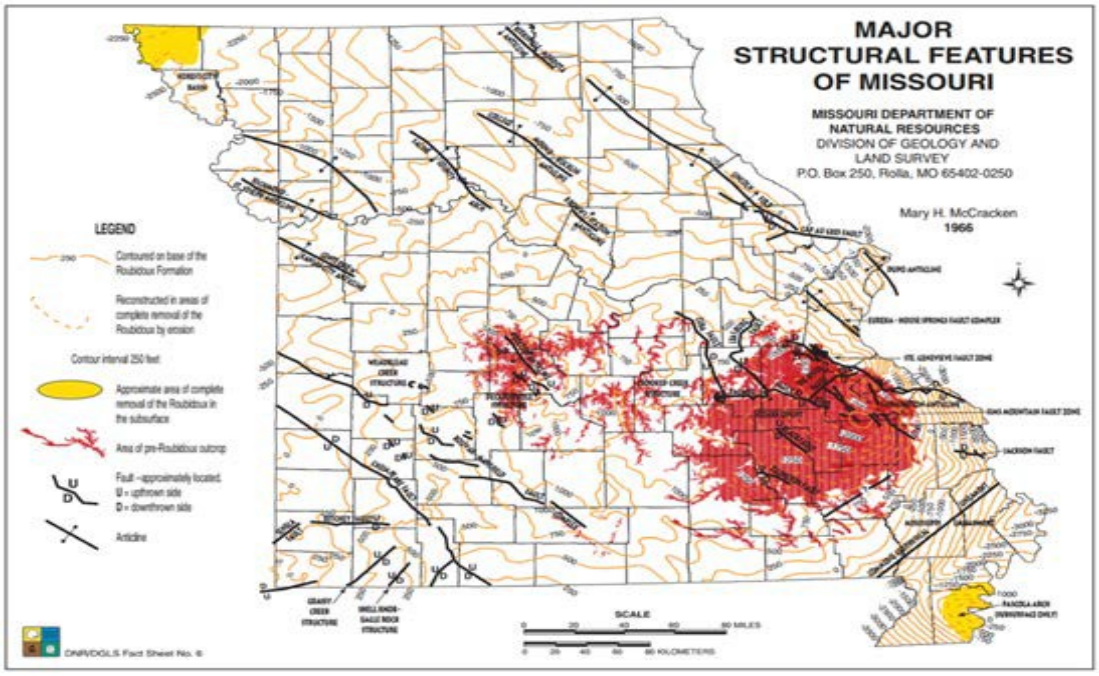

Figure 3.3. The faults observed in Greene County trend NE and NW (McCracken, 1966).

3.2 BEDROCK STRATIGRAPHY

The three main stratigraphic systems of the Springfield Plateau bedrock are detailed in Table 3.1. The three systems are the Cambrian, Ordovician, and Mississippian. The Upper series of the Cambrian consists of six formations beginning with Lamotte Formation, an approximately 150 ft unit consisting of quartz sandstone. Overlying the Lamotte formation is the Bonneterre Formation, an approximately 200 ft unit of medium to fine-grained dolomite. Overlying the Bonneterre Formation is the Davis Formation, an approximately 150 ft shale unit intermixed with dolomite.The Derby-Doerun, Potosi, and Eminence Formations conclude the Cambrian System in the

Springfield area. These formation are characterized by clean dolomite with a small amounts of chert and comprise a total thickness of approximately 500 ft.

The Cambrian System in the study area is overlain by the Ordovician System, which is represented by the following geologic units: Gasconade Formation, Roubidoux Formation, Jefferson-City Formation, and Cotter Formation. The basal unit in the Ordovician System, the Gasconade Formation, is comprised of three members: Gunter Sandstone, Lower Gasconade Dolomite, and Upper Gasconade Dolomite. The total thickness of the Gasconade Formation is approximately 375 ft, and it is mostly comprised of interbedded sandy dolomite, cherty dolomite, and quartz sandstone. The Gasconade Formation is overlain by the Roubidoux Formation. With a thickness of 150 ft, this formation mostly consists of dolomite, but has some inclusions of chert.

In some locations, the Roubidoux Formation is interbedded with layers of sandstone. Due to climatic changes in the region, carbonate rocks became predominant after the Roubidoux Formation. The deposition of Ordovician Age rocks continued with the deposition of two more Formations: Jefferson-City and Cotter. The total thickness of these two Formations is approximately 600 ft (Bullard et al., 2001).

The Ordovician System is overlain by the Mississippian System, which in Greene County is represented by the Compton, Northview, Pierson, Reeds Spring, Elsey, and Burlington-Keokuk Formations. The total thickness of this system is about 640 ft. The Mississippian System starts with the Compton Formation, which has a thickness of less than 30 ft. The Compton Formation is overlain by the Northview Formation with the average thickness up to 80 ft. The Mississippian System continues with the deposition of the Pierson, Reeds Spring, and Elsey Formations. The total thickness of these three

formations is about 260 ft. Cherty limestone is a dominant component in all three formations. The deposition of the Mississippian System is finalized by the Burlington-Keokuk Formation, the youngest rock unit exposed in Greene County. The thickness of the formation is approximately 270 ft and it consists of fossiliferous limestone and cherty limestone. The majority of karst features in Greene County are found in Burlington-Keokuk Limestone.

Table 3.1. Geologic and stratigraphic units in the study are (Vandike, 1993).

System	Series	Group	Formation		Thickness (ft)
Mississippian	Osagean		Burlington- Keokuk Formation		150-270
			Elsey Formation		25-75
			Reeds-Spring Formation		125
			Pierson Formation		90
	Kinderhookian	Chouteau	Northview Formation		5-80
			Compton Formation		30
Ordovician	Canadian		Cotter Formation		600
			Jefferson-City Formation		
			Roubidoux Formation		150
			Gasconade Formation	Upper Gasconade Dolomite	350
				Lower Gasconade Dolomite	
				Gunter Sandstone Member	25
Cambrian	Upper		Eminence Formation		500
			Potosi Formation		
		Elvins	Derby-Doerun Formation		
			Davis Formation		150
			Bonneterre Formation		200
			Lamotte Formation		150
Precambrian	Crystalline rock				

4. KARST

4.1 THE DEVELOPMENT OF KARST FEATURES

A range of diverse engineering and environmental issues typically develop in regions in which natural geological substrates are exposed to erosion. Such issues can lead to the development of voids below the surface of the rock. These voids are often referred to as karst features. “Karst” is a distinctive form of landscape that evolves as a result of water dissolving the bedrock primarily impacting soluble bedrock such as halite, limestone, dolostone, and marble. Landscapes that contain karst are dotted with sinkholes, caverns, springs, shafts, and caves. They have unique features that are the result of an intricate interaction of hydrology, geology, topography, climatic, and biological factors. Karst features can be found at all elevations and altitudes. Rocks that contain some form of karst features currently cover an estimated 20% of the surface of the Earth (Ford & Williams, 2007). The primary features of Karsts were documented by the American Geological Institute (AGI) and are presented in (Figure 4.1) (Veni et al., 2001).

As can be observed in Figure 4.2, Missouri is predominantly underlain by carbonate rocks that are host to many karst features, as the majority of Missouri’s counties sit on carbonate rock units. Significant karst development has emerged in the southeastern and southwestern areas of Missouri due to the fact that the carbonate rocks in these areas are more exposed and sit under permeable rock units.

The karst features highlighted in a dark green color are predominantly formed on the subcropping carbonate rocks. The buried carbonate rocks are depicted by a light green

color. The light blue color characterizes covered evaporate rocks (gypsum and halite), and dark blue depicts the exposed rocks. The red and yellow represent pseudo karst; of which red is volcanic and yellow is formed of unconsolidated material (Veni et al., 2001).

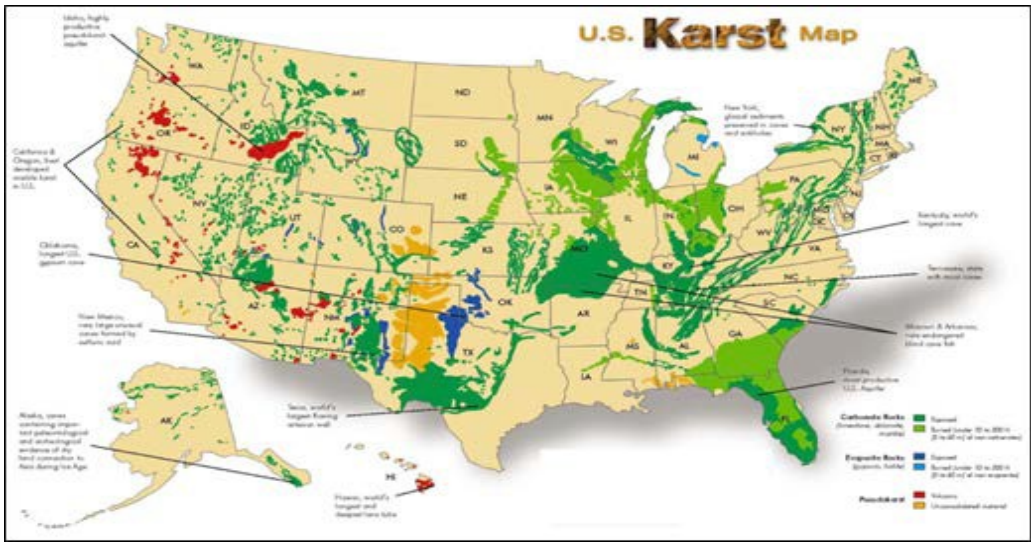

Figure 4.1. The distribution of Karst features in the US (Veni et al., 2001).

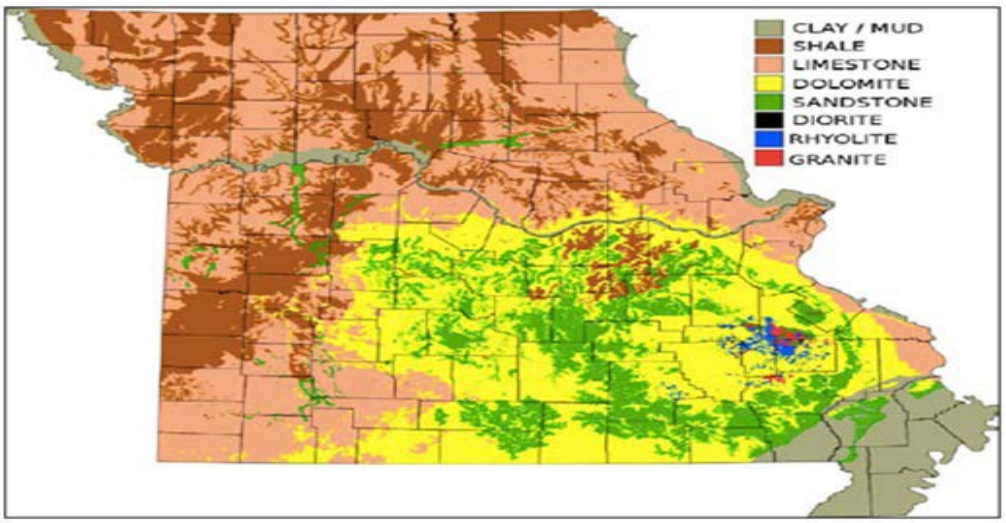

Figure 4.2. The distribution of rock units in Missouri. (Source: http://upload.wikimedia.org/wikipedia/commons/a/a1/Missouri_Geology Primary_Rock_Types_v1.png).

4.2. KARST FORMATION

Karst features are formed in carbonate rocks when acidic rainwater penetrates through the fractured/jointed rock and react with carbonate minerals such as calcite (CaCO3) and dolomite (CaMg [CO3] 2) which results in the dissolution of carbonate rocks. Limestone dissolution can be described by the following reactions:

$$H_2O + CO_2 \rightarrow H_2CO_3$$

$$CaCO_3 \rightarrow Ca^{2+} + CO_3^{2-}$$

$$CO_3^{2-} + H_2CO_3 \rightarrow 2\,HCO_3^{-}$$

$$CaCO_3 + H_2CO_3 \rightarrow Ca^{2+} + 2\,HCO_3^{-}$$

According to Jennings (1966) and White (2002), smaller features of karst are observed in lithified carbonate rocks than those of weaker carbonate rocks. The cracks and joints that form throughout the bedrock and soil allow the water to pass below the surface to form a zone in which the voids and fractures fill with water, the volume of which varies according to the rock porosity. The more significant the fraction of voids that exist in an area of rock or soil, the greater its porosity. When the voids start to join, air and water can move from one void to another, making the bedrock or soil permeable. Permeable bedrock is an effective aquifer because the layer of rock is able to store and conduct water. If acidic groundwater flows within the underlying permeable bedrock and this bedrock is soluble, the distinct karst topography can emerge (Figure 4.3).

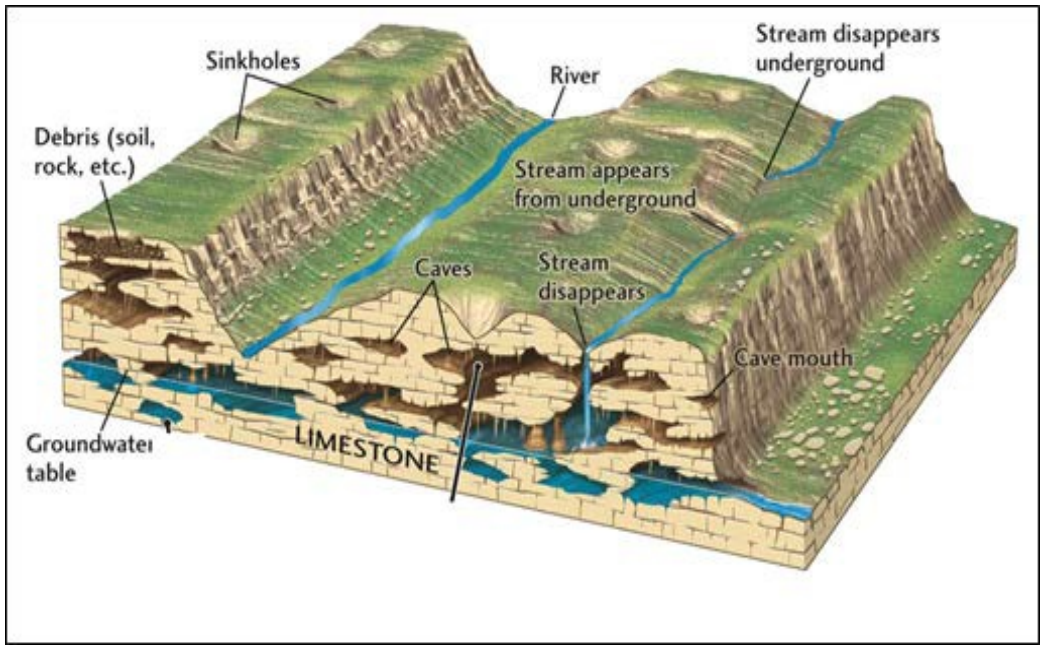

Figure 4.3. Landscape presenting the karst features (https://cetologydotorg.files.wordpress.com/2015/01/karst_topography.jpg).

The climate of a given region has a strong impact on the formation of karst as it directly influences the amount of water that flows through the region. The availability of biogenic carbon dioxide has a direct impact on the extent to which the calcium carbonate dissolves in contact with the water. High concentrations of biogenic carbon dioxide are found in deep soils and tropical zones. In these areas, the organic matter is rapidly decomposed and, as such, the most developed karsts are typically found in wet tropical environments.

Less dissolution of limestone is observed in temperate areas, and less still in arid glacial locations. The dissolution that is observed in Missouri frequently takes place through joints that are in-filled with piped fine-grained sediments, such as silts and clay.

These are eroded and pass down into the rock via the water that infiltrates the solution-widened joints.

The features of karsts can range from microscopic chemical precipitates through to massive ecosystems and drainage structures that span hundreds of square miles.

4.3. THE DEVELOPMENT OF KARST SYSTEMS

The way in which a karst system develops and its resulting magnitude ranges according to a wide range of factors. Those factors include but are not limited to the following: the nature and form of the carbonate formations, the extent to which these formations are impacted by jointing and fracturing, the thickness of the carbonate, and the topographic setting. Two fundamental elements that directly impact the intensity and degree of karst development are weathering and environmental conditions. Areas that have acidic rainfall and subsurface flow in combination with extensive and intensive and fracturing and jointing have favorable conditions for significant development of extensive and intensive karst features. The karst features that can be currently found in the southwest area of Missouri can be traced back to the humid weather conditions that were dominant in previous geological eras.

4.3.1 Sinkhole Formation. The U.S. Geological Survey has recorded in the region of 15,981 sinkholes in Missouri, with in excess of 2500 of these being present in the southwestern region as well as 245 caves (Greene County Comprehensive Plan, 2007). Groundwater that is slightly acidic passes through the fractures and joints in bedrock. As it does so, it gradually dissolves the carbonate rock to form solution- widening joints. In locations in which perpendicular intersecting sets of joints are located in close proximity to one another, the solution widens the joints, resulting in the formation of columns of bedrock separated by narrow joints. These geological features are referred to as pinnacles. As the rocks dissolve, the roof thins, leading to the

subsidence of the overlying soil. The roof eventually collapses, leading to the development of a steep-sided cone-like shape that points inward. These features are referred to as collapse sinkholes and the associated features are known as solutional sinkholes (Figure 4.4).

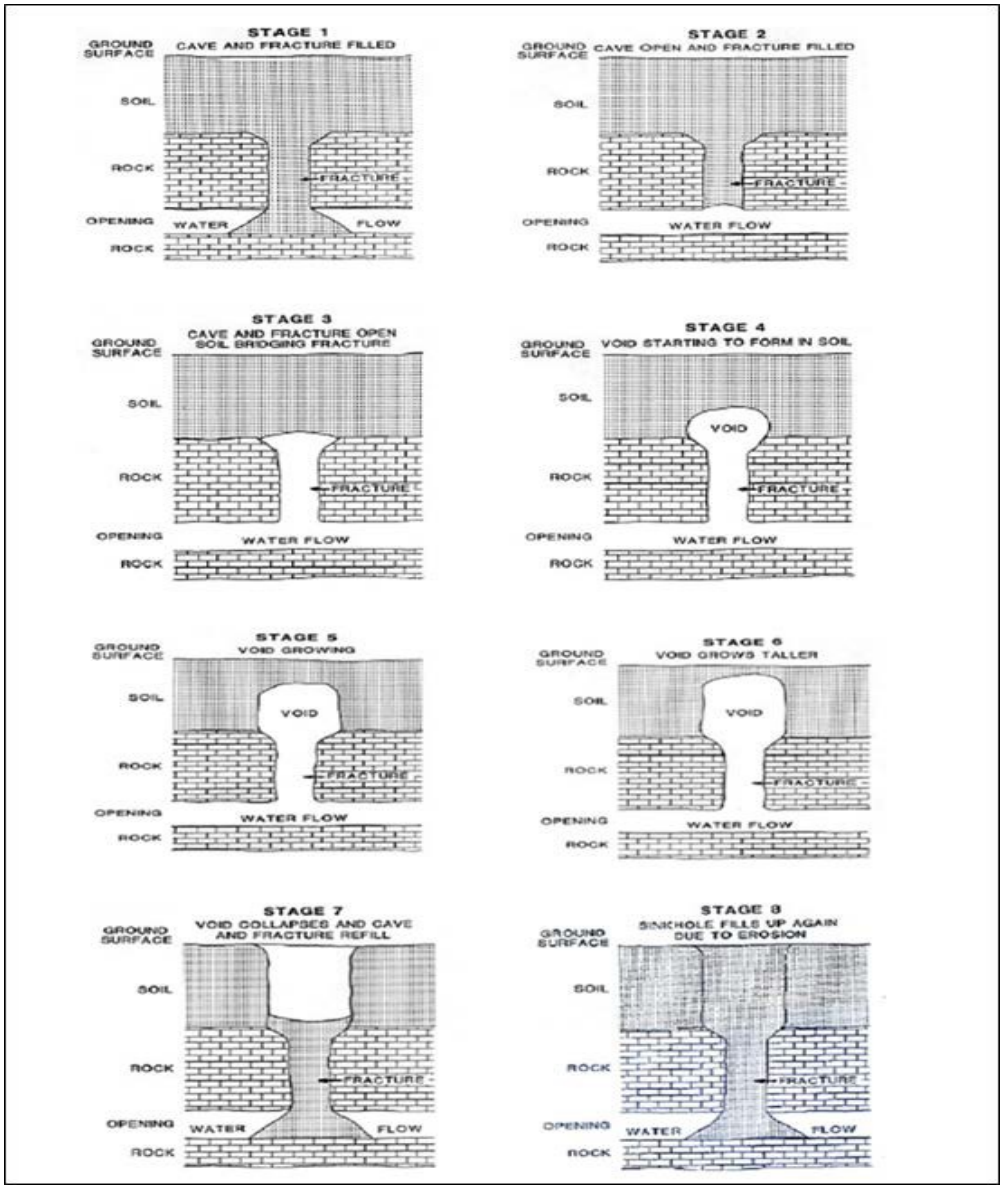

Figure 4.4. Illustrates how stages of a sinkhole formation.

4.3.2 Types of Sinkholes. Three engineering examples of naturally occurring sinkholes will be described in this section: solution sinkholes, cover-collapse sinkholes and cover-subsidence sinkholes.

4.3.2.1. Solution sinkholes. Solution sinkholes are smaller, more shallow formations occurring where metamorphic and sedimentary rocks (e.g. limestone and dolostone) are bare or only partially covered by permeable soil or sand. Dissolution occurs along limestone fractures, joints, or similar openings in the rock permitting water to easily move below the surface. While rain falls and collects on the surface, water will begin to percolate through joints in the limestone or dolostone leaving the dissolved rock to be carried away from the surface allowing a small depression to be formed. Draining continues on the rock surface accelerating the dissolution process and causing the depression to enlarge while water outflow may remain forming a pond which allows water to remain over time. However, solution sinkholes rarely collapse and pose no threat to the environment. (Figure4.5)

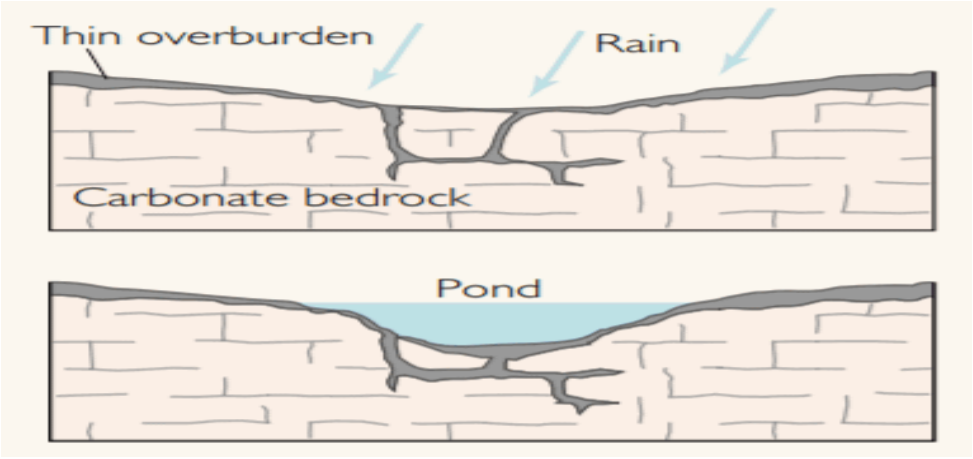

Figure 4.5. The development of solution sinkhole. (USGS).

4.3.2.2. Cover-subsidence sinkholes. Cover-subsidence sinkholes tend to develop gradually and where the covering sediments are permeable and contain higher percentages of sand. In areas where cover material is thicker, or sediments contain more clay, cover-subsidence sinkholes are relatively uncommon, are smaller, and may go undetected for long periods. The formation occurs due to piping, a process where limestone dissolves, causing sand to move downward occupying the void created by the dissolving limestone. The dissolution causes a depression in the surface area. Where limestone is covered beneath thick, unconsolidated material, fewer sinkholes occur. Low permeability may impede movement of surface water and slow the development of solution cavities in the subsurface limestone. (Figure 4.6)

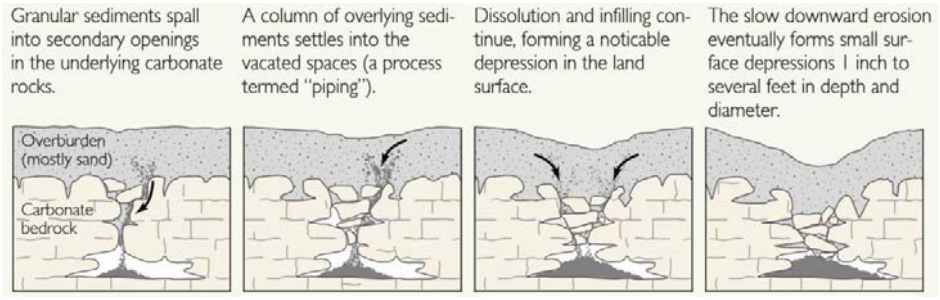

Figure 4.6. Development Cover-subsidence sinkholes. (USGS).

4.3.2.3. Cover-collapse sinkholes. Cover-collapse sinkholes occur where the covering sediments contain a significant amount of clay. Over time, surface drainage, erosion, and deposition of sinkhole into a shallower bowl-shaped depression. Cover-collapse sinkholes are often circular with steep-sloping sides. Cavity formation is caused by surface water filtering through spilling sediments continuing to collect and create a

cohesive cover. The collections of material begin to form a structural arch and the cavity enlarges to the point to where the cover material is unable to continue bearing its own weight culminating in a sudden collapse. This sinkhole can be triggered by incessant rainfall, extreme drought or mechanical. The collapse is abrupt, and often catastrophic. (Figure4.7)

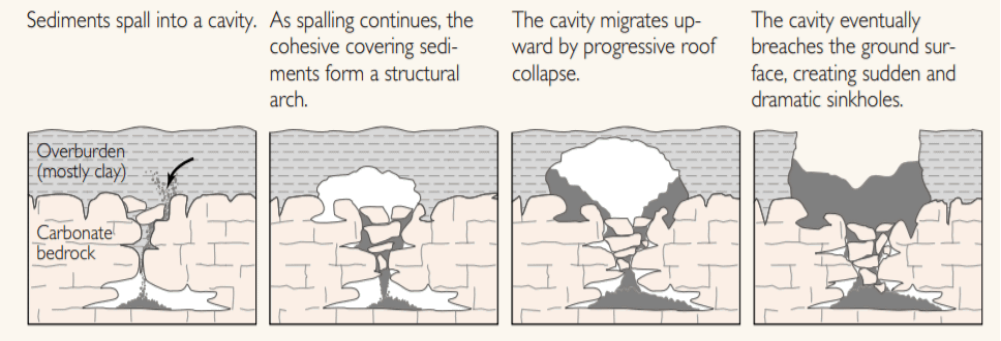

Figure 4.7. Development Cover-collapse sinkholes. (USGS).

4.3.3. Anthropogenic Sinkholes. Subsidence can also occur artificially as a result of excessive rain, stormwater drainage and engineering structures. Most sinkhole develop as naturally occurring karst processes, however; sinkholes maybe engineered through mishap or poor planning. The natural occurrence of developing sinkholes may be described thus far as the slightly acidic groundwater seeping into the natural fractures in the rock. Similarly, the process can be facilitated by increasing the dissolution rate of bedrock and/or by reducing the ability of the underground cavity to support the taxing burden created by anthropogenic activities and structures. It is important to understand that karst processes that naturally occur may be unable to be prevented, but human activities that cause sinkholes can be minimized to prevent catastrophic sinkhole

formations. Kochanov (1999) discusses activities caused by human engineering that can often lead to the triggering of deadly sinkholes. For example, when the water table is lowered due to excessive withdrawal of groundwater, the pressure in the soluble bedrock is weakened considerably thus reducing its cavity capacity and ability to support the taxing burden often leading to sudden collapse as seen in most collapse sinkholes.

Other factors that may lead to sinkholes include, but are not limited to urbanization and overpopulation. Overtaxed human constructed drainage systems frequently supply a high concentration of surface water to areas, which cannot support the rapid absorption (e.g. the weathered bedrock). The exposed bedrock is then bombarded by large amounts of water and cannot support the fast rate of dissolution because of its high solubility. Many engineered structures pose a danger to the area's stability due to being constructed near or over undetected voids, thus creating a large amount surface mass with inevitable consequences.

4.3.4. Sinkholes in Missouri. In Missouri the majority of sinkholes are occurred when surface water seeps through the fractured rocks or anthropogenic passageways (i.e. drainage structures, roads, buried pipes); and transfers particles of clay that fill the joints. This process is called "piping". As water and clay particles seep into the subsurface they create a passageway or "soil pipe", this enlarges subsurface pathways due to the increased erosion. The increased erosion creates voids that eventually cannot support the overlying ground surface resulting in subsidence and sometimes collapse. While soil piping is a natural process, anthropogenic activities increase the risks, especially in karst regions such as Missouri (Schneider, 2014).

5. METHODOLOGY

A brief review of the different methods used in this research will be demonstrated in this section. Tow geophysical tools were used, the electrical resistivity tomography ERT, and multichannel analysis of surface waves. The description of the methods will be detailed. Beginning with the basic theory beyond the technique and going through data acquisitions, data processing, and data interpretation.

5.1. ELECTRICAL RESISTIVITY TOMOGRAPHY (ERT)

The electrical resistivity tomography ERT is a nondestructive geophysical method that measures the spatial differences in the resistivity of the earth materials such as soil, rock, and water in the subsurface. The electrical resistivity method is an appropriate tool that uses in hydrogeological, mining, geotechnical, and more recently environmental investigations (Loka, 2011). The aim of using the electrical survey is to determine the distribution of subsurface resistivity by obtaining measurements on the ground. Each one of those materials has elements in varying degrees of resistivity. Also, The ERT method is extensively used as the conventional geophysical tool for investigating the depth of bedrock and areas of subsurface dissolution. For these reasons, the ERT is considered to be an appropriate geophysical method in characterizing the karst terrain features.

5.1.1. Basic Theory of Electrical Resistivity. Conceptually, the electrical resistivity survey is relatively straightforward. Ohm's law represents the fundamental physical law that used in electrical resistivity surveying. By using Ohm's law equation (showing below) the resistance can be calculated. Where V is the applied voltage or electromotive force, *I* is the current flow and R is circuit resistance.

$$V = IR \qquad (1)$$

The difference between resistance and resistivity, a unit cylindrical (Figure 5.1).

$$\rho\rho = \partial RR\frac{\partial A}{\partial L} \qquad (2$$

Where **ρ** is the resistivity of the material the object is made of, **l** is the length of the material **A** is the cross-sectional area the current flows through.

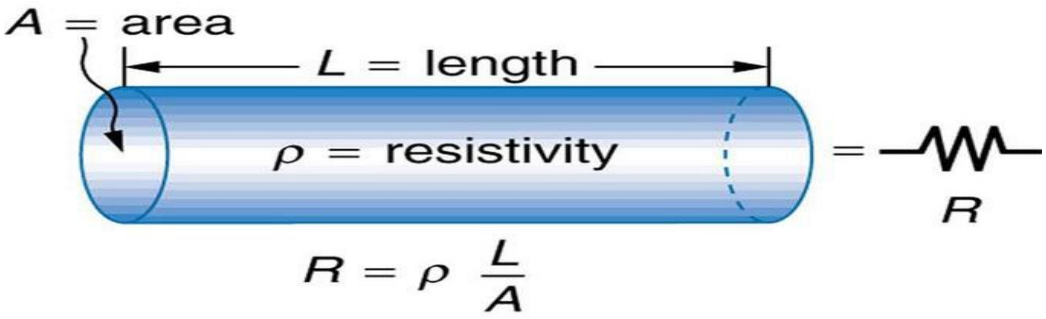

Figure 5.1. Resistivity parameters for a conducting cylinder. (https://courses.lumenlearning.com/boundless-physics/chapter/resistance-and-resistors/)

5.1.2 The Relationship between Geology and Resistivity. Fluctuations in resistivity of materials below the surface is referred to as lithology. Information about fluctuations in resistivity can be accredited with different below surface materials. A few materials that indicate resistivity (Figure 5.2) and/or possible superposition in the values of resistivity in different materials require further gathering of information in order to confirm material types e.g. minerals which tend to be insulators rather than conductors,

resistive. For rock formations further from the surface, conduction is assisted via ions in pore fluids, an electrolytic conduction which is the inverse of resistivity. This type of conduction is affected mostly by porosity, salinity, lithology, and saturation as well as by clay content and somewhat by temperature.

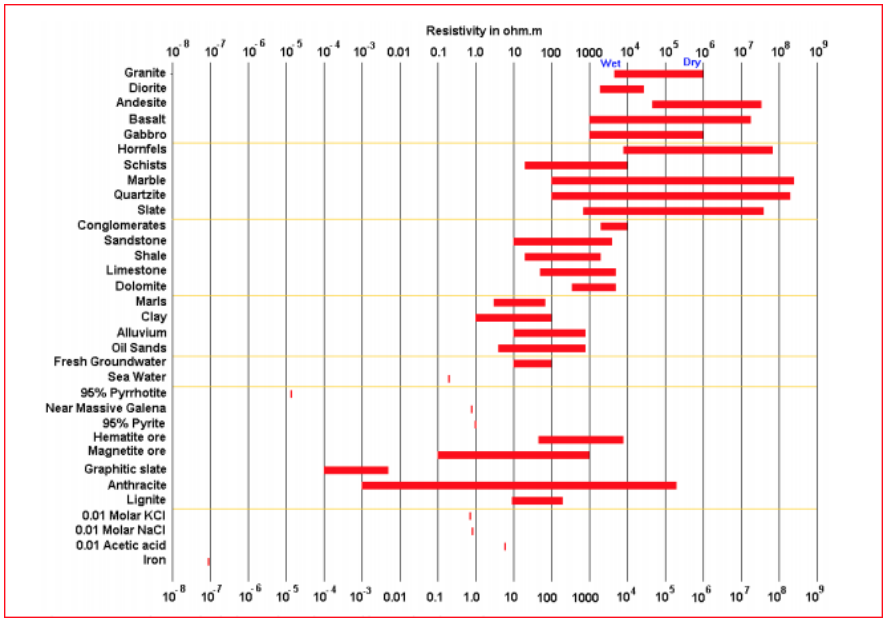

Figure 5.2 Relationship between geology and resistivity.

5.1.3. Electrical Resistivity Arrays. Most often electrical resistivity tomography surveying is done with one of the electrode geometries more commonly known e.g. Schlumberger array, Wenner array and Dipole-dipole. Electrode configurations, the general arrangement of current and potential electrodes (Figure 5.3) show potential conductivity when placed between the current electrodes. Dipole-dipole electrode array (Figure 5.4.) were more commonly used in the study because of its good coverage of karst terrain, which is mostly high and variable laterally. Typical depths of investigation were generally around 20% length of the array. As for electrical resistivity tomography

(ERT) survey, availability of the area for the survey, in order to avoid trespassing, depth of the area under investigation and, of course, the number of electrodes available are all factors that are considered before commencing a survey (Obi,2016).

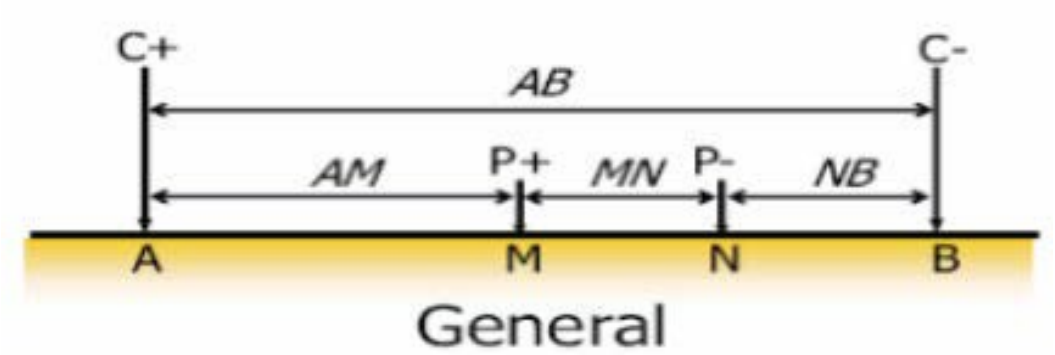

Figure 5.3. Potential conductivity when placed between the current electrodes.

Figure 5.4. Dipole-dipole electrode array.

5.1.4. ERT Data Acquisition. To acquire ERT data involves using the SuperSting resistivity meter or control unit which is powered by one or two 12-Volts

batteries is used to inject a single electric current into the ground via electrodes. Electrode cables are firmly fastened to metal stakes which are then pounded into the ground using springs or rubber-bands during the set-up process. The electrodes may also be connected to a switch box in order for connection to the resistivity meter (passive electrodes). A laptop can be used to download or upload data to the SuperSting, as well as be connected to the SuperSting during data acquisition or for later during data processing and transfer. Four electrodes are normally used at each point of entry: for injecting current into the ground, two current electrodes; and for measuring the resulting voltage difference two potential electrodes (Obi,2016) .

Apparent resistivity is calculated as a weighted average of different resistivities under the four electrodes from which the resulting voltage and current are measured. Should the ground be homogeneous, the apparent resistivity will equal the true resistivity. However, most often, dipole-dipole array would be used because it is the most convenient array, logistically, in its field, especially for larger scale projects. In dipole- dipole array, a multi-core cable is attached to the electrodes in a straight configuration and is then connected to the switching unit, which is directly hardwired into the SuperSting resistivity meter. This particular array controls the selection of the A&B current and M&N potential electrodes for each measurement. It is worth mentioning that acquisition time for a dipole-dipole array using 72 electrodes can take more time, approximately 45 minutes to two hours for 84 electrodes and as much as three hours for 168 electrodes upon completion of the survey set-up. Depth of Investigation for a dipole- dipole array is about 20% -25% of the length of the array. It was the dipole-dipole electrode array (Figure 5.5) and (Figure 5.6.) which was used throughout this study.

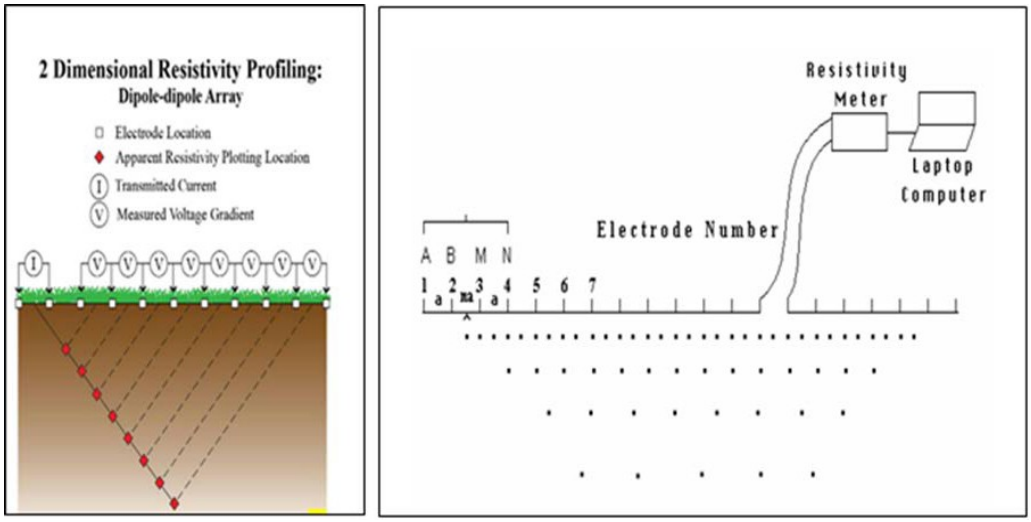

Figure 5.5 .The particular array controls the selection of the A&B current and M&N potential electrodes for each measurement.

Figure 5.6. The field equipment of the ERT.

5.1.5. ERT Data Processing. The software program used for this study to convert the apparent resistivity data to true resistivity (inversion) was RES2DINV. Once ERT data was compiled, then the first step in processing raw data was the elimination the bad data (Figure 5.7.) represented by values of high or low resistivity. Several factors can account for inferior data, e.g. equipment malfunction, electrodes to ground contact caused arid soil or shorting across the cables or sodden ground conditions (Obi, 2016). At this point, resistivity imaging (2D) is generated of the subsurface which represents resistivity of the area (true form) thus revealing the distribution of resistivity across a traverse as shown in (Figure 5.8). During data processing, it is imperative that the root mean square (RMS) error to be within a certain range, for example 5% is considered an acceptable geologic model (Nwokebuihe, 2014) (Loke,2011)

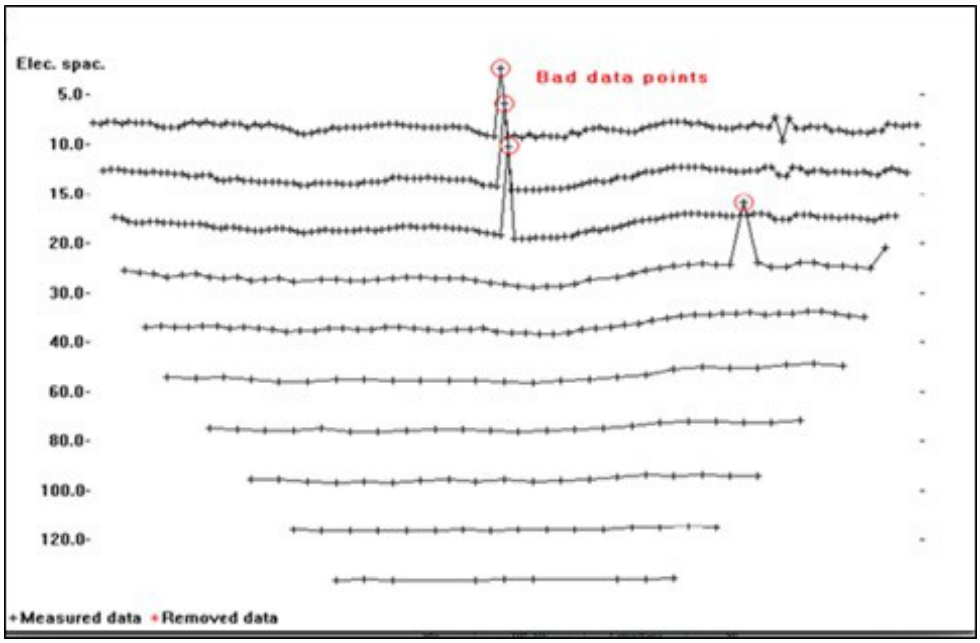

Figure 5.7. The elimination the bad data represented by values of high or low resistivity.

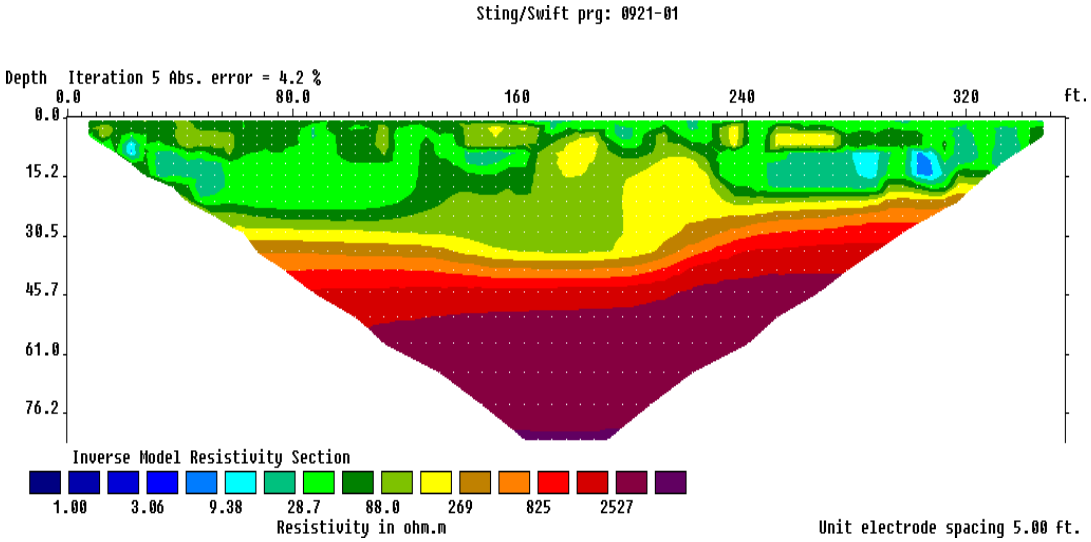

Figure 5.8. Revealing the distribution of resistivity across a traverse.

5.1.6 ERT Data Interpretation. As depicted by Table 5.1, resistivities are vastly different when comparing soil samples of voids, cavities, soil, weathered rock, and intact rock. Different factors can affect the electrical current flow, e.g. salinity, porosity, saturation, and lithology, as well as clay content, and temperature of the material composition may force the electrical current to be subverted due to electrolytic conduction. Hence, Variables of mineral composition may present a variance in resistivity values. For example, soil that is less dry usually has a higher resistivity than soil that is saturated. The same scenario may play out with weathered rock which tends to be more porous or fractured causing it to become saturated with groundwater in contrast to unweather rock which does not. As a result, weathered rocks have a much lower resistivity than intact rocks. According to Anderson (2006) who also conducted research in Southwest Missouri found similar results. The moist clays are characteristically noted

for lower values of resistivity typically under 100 ohm-m, and often fluctuate because of varying degrees of limestone porosity, and saturation due to ground cover. The moist soil mixed with significant amounts of fractured rocks and clay exhibit higher resistivity values and are usually between 100 and 400 ohm-m, but also may produce a variance because of differing degrees of porosity, and saturation due to ground cover. The two areas that showed the highest resistivity values were the non-fractured limestone with less clay content with values of more than 400 ohm-m resistivity, and the cavities with more than 10000 ohm-m. This can be explained by noting the varying thickness of the intact limestone and its porosity, moisture present, saturation levels, and a variety of impurities. The cavities, typically air-filled, exhibit higher resistivity values possibly due to their depth, size, and shape of the void, as well as for the surrounding strata. (Anderson et al., 2006) The area was most typically intact bedrock, but covered by layers of moist loose materials like clay. However, areas, such as air-filled pockets are found in non-fractured limestone, are areas noted for their contrasting electrical resistivity.

Table 5.1. Resistivity are vastly different when comparing soil samples of voids, cavities, soil, weathered rock, and intact rock.

Earth Material	Resistivity, Average or Range (Ohm-m)
Moist Soil	<125
Dry Soil	> 125
Moist weathered and/or fractured rock	<600
Fractured rock with moist piped clay-fill	< 125
Intact rock	>600

5.2. MASW METHOD

MASW is a geophysical tool that determining the acoustic properties of soil/rock and estimating the top of rock is progressively used to inspect complex karst terrain (Bansah et al., 2017). The active MASW tool is a seismic method for determining the hardness of soils and/or rock in the subsurface for different aims such as geotechnical, geophysical and geological engineering. The purpose of using MASW In this research is to provide additional accuracy to (ERT) interpretations.

5.2.1. MASW Data Acquisition and Processing. (Figure 5.9.) Shows the field equipment that used to acquire MASW data. The source that usually used to acquire data is sledgehammer (usually 20-lbs.), receiver or geophone, seismograph, battery, impact plate, cables, connectors and a computer laptop. After striking the hammer, the recorded data on the seismograph is transformed to a laptop computer. When data acquisition is done field data can be analyzed by using Surfseis software. There are two steps to process the MASW. The first step is arranged the fundamental-mode dispersion curves, and then inverting these curves to generate 1-D shear wave velocity profile (Figure 5.9). This shows depth vs shear wave velocity relationship in linear form.

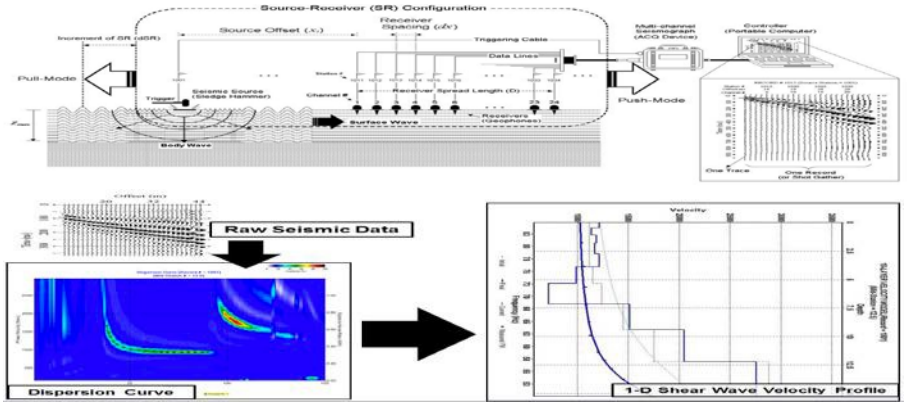

Figure 5.9. The field equipment that used to acquire MASW data.

5.2.2. MASW Data Interpretation. To better understand S-wave propagation is important as it relates to the properties of the materials. One example is material such as soil, which has a lower S-wave velocity than competent rocks. In any given sinkhole study this scenario may play out differently due to the dissolution of the bedrock containing depressions, collapsed shallows or filled with surficial deposits where lower S-wave readings are expected especially when compared to the surrounding competent rock. The National Earthquake Hazard Reduction Program(NEHRP) area classifications chart indicating a variety of geological materials published by the International Building code in 2000 (Table 5.2). This table indicates a base of classification of subsurface materials based on their values of shear wave where 1000 - 1200 ft/sec is most often interpreted as the shear wave velocity correspondence to limestone bedrock surface area.

Table 5.2. This table indicates a base of classification of subsurface materials based on their values of shear wave.

Site Class	Soil Profile Name	Average Properties in Top 100 feet (as per 2000 IBC section 1615.1.5) Soil Shear Wave Velocity, V_s	
		Feet/second	Meters/second
A	Hard Rock	$V_s > 5000$	$V_s > 1524$
B	Rock	$2500 < V_s \leq 5000$	$762 < V_s \leq 1524$
C	Very dense soil and soft rock	$1200 < V_s \leq 2500$	$366 < V_s \leq 762$
D	Stiff soil profile	$600 < V_s \leq 1200$	$183 < V_s \leq 366$
E	Soft soil profile	$V_s < 600$	$V_s < 183$

6. GEOPHYSICAL STUDY

In this research, different tools were expounded to describe and investigate several features in the study area in Greene County southwestern Missouri. The preliminary site studies and geophysical studies were done. The preliminary site study was included aerial photographs. These aerial photographs were downloaded from google earth to provide a good overview of the site. The aerial photographs divided into four parts because the survey cover large area (Figure 6.1 - 6.4).

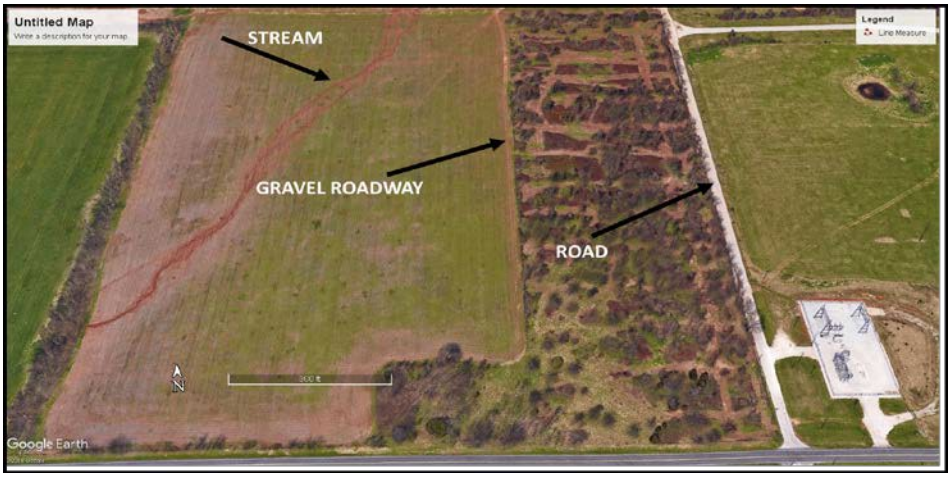

Figure 6.1. Aerial photograph of the study area part one (the distance in feet).

As can be observed in the four aerial photographs the site includes parking lots, roads, streams and hedges. In this section, the impact of these features will be discussed. The two geophysical methods were involved; the electrical resistivity tomography (ERT), and the multichannel analysis of surface waves (MASW). These tools were explained in this study to identify and assess the possible karst development in the location. This study aimed to determine the depth of the top of rock, observing the groundwater flow, and study the characteristics of the rock. Eight ERT profiles oriented west-east were acquired

in this study site. (Figure 6.5.) Shows the ERT profiles locations (labeled T1, T2, T3, and T4 to T8) and seven MASW profiles were linked to ERT (T1) (labeled M1, M2, to M7). The maximum depth of each ERT profiles was (100ft), and the length of the profiles was approximately (4780ft) with (5ft) intervals electrodes intervals.

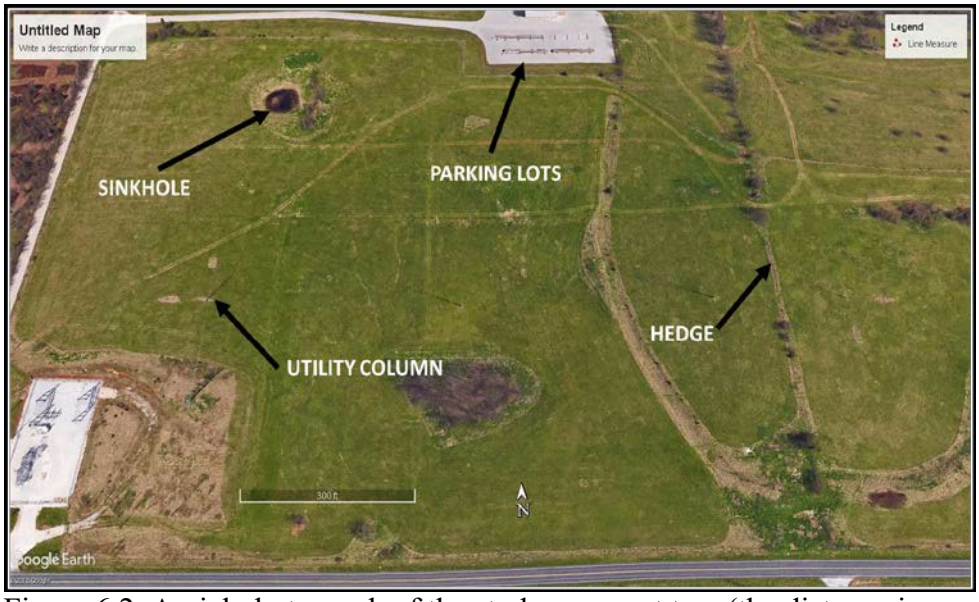

Figure 6.2. Aerial photograph of the study area part two (the distance in feet).

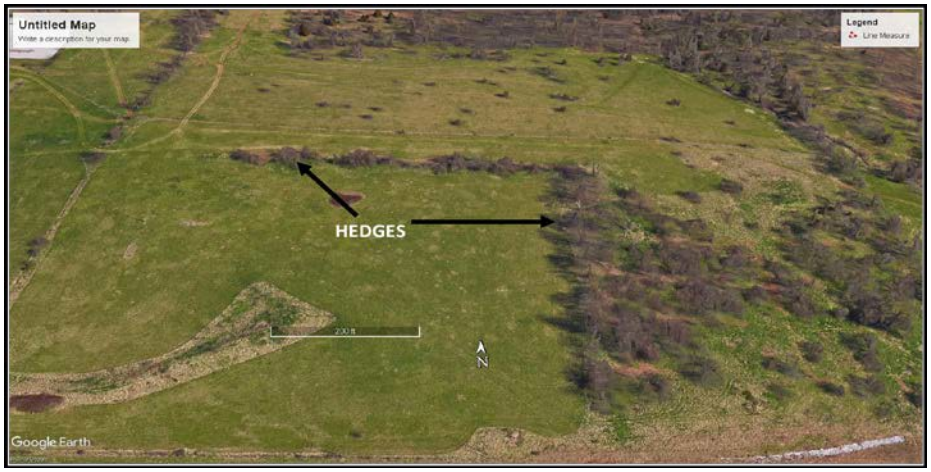

Figure 6.3. Aerial photograph of the study area part three (the distance in feet).

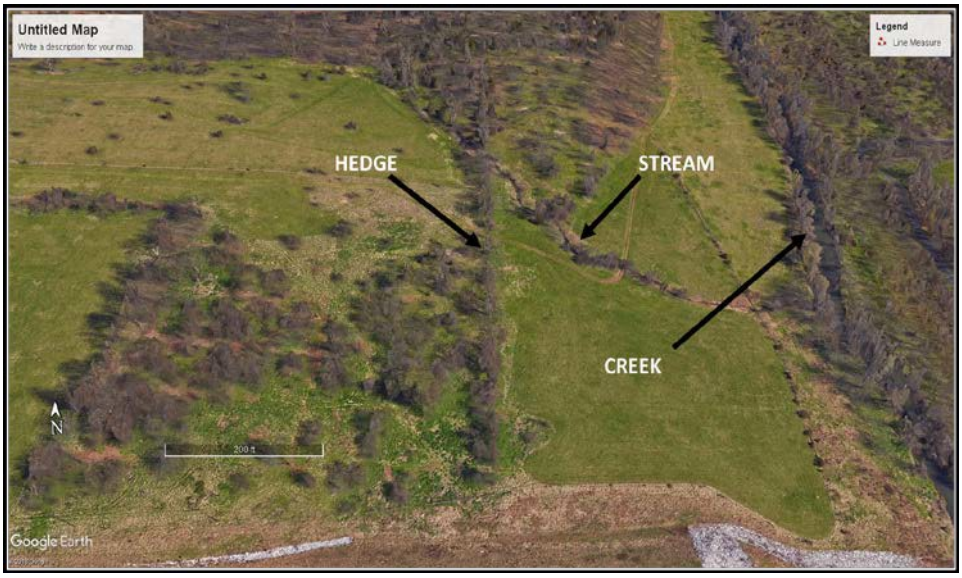

Figure 6.4. Aerial photograph of the study area part four (the distance in feet).

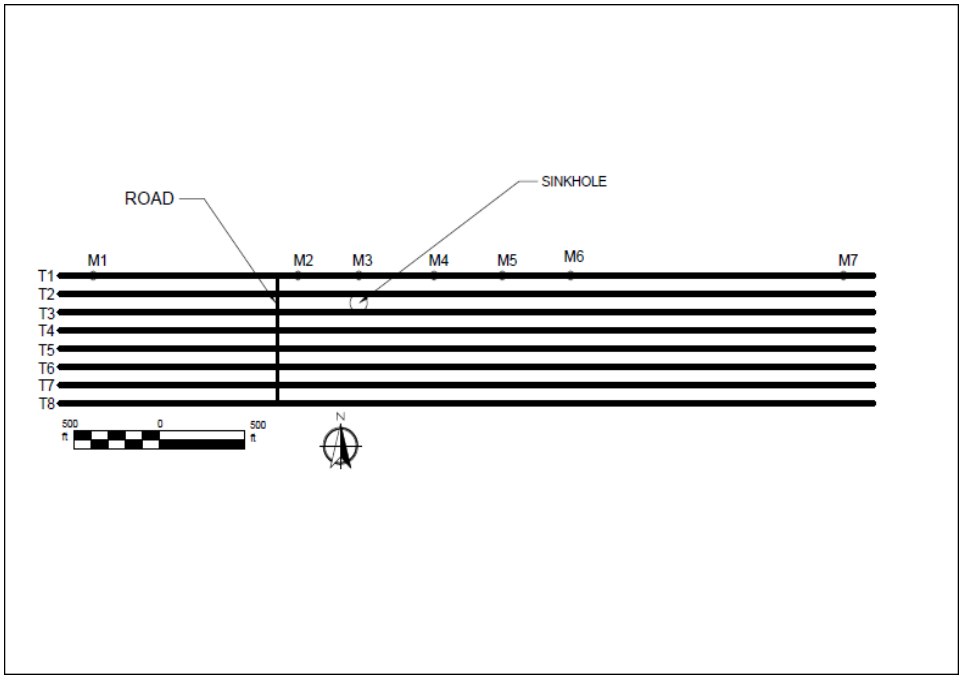

Figure 6.5. The location of electrical resistivity tomography ERT and Multichannel Analysis of Surface Waves MASW on the site.

Surface elevation contour map illustrates the directions of the surface drainage pathways (Figure 6.6.) as can be observed in the figure the drainage pathways have multi-directions. The main direction is north south.

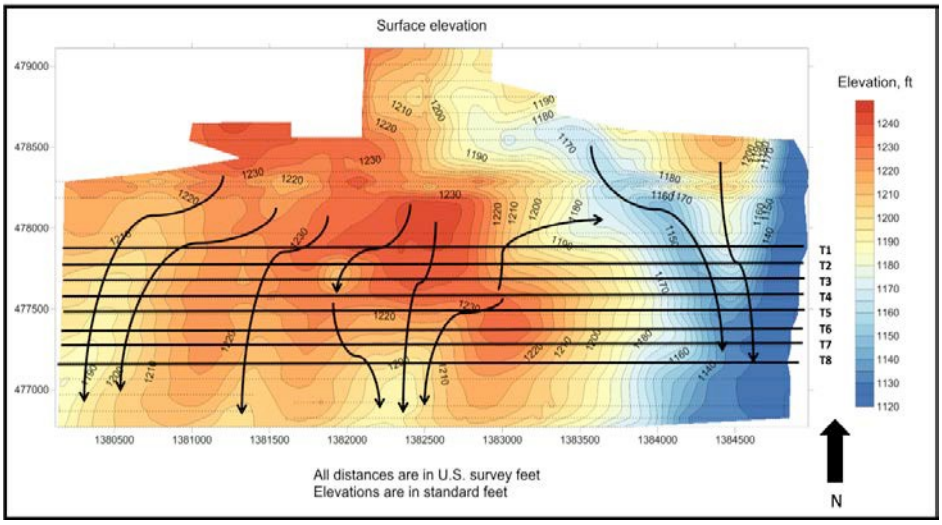

Figure 6.6. Surface elevation contour map illustrates the directions of the surface drainage pathways.

6.1. ERT DATA INTERPRETATIONS

The ERT interpretations can be divided into four categories as following, dry soil, moist soils, moist rock, and dry rocks. These divisions connected to the differential in moisture contents in the rocks. Consequently, the resistivity values greater than 125 ohm-m is represented the moist rocks and dry soil while the resistivity values less than 125 ohm-m represented the moist soils and greater than 600 ohm-m is represented as a dry rock.

6.1.1. Top of The Bedrock. Based on the interpretations of the acquired ERT data the depth to the bedrock has been determined (demonstrated by the black line in the Figures 6.7…6.14). The depths to the bedrocks are approximately as shallow as 3 feet

and as deep as 40 feet. According to the acquired ERT data, the bedrock has approximately 125 ohm-m resistivity values. The interpreted ERT data showed that there are many low resistivity zones were observed in the study area these zones of low resistivity zones reflected the variations in the moisture content.

6.1.2. Anomalies Zones. Based on the interpretation of the acquired ERT profiles, the rock beneath the study area is significantly fractured. There are many anomalies zones were found in in the subsurface. These anomalies zones observed in most ERT profiles due to the high conductivity of the moisture content as a result of both man-made and natural factors.

In ERT T1, eight anomalous zones were identified. They labeled by letters A, B, C, D, E, F, G, and H. As can be observed in the aerial photographs (Figure 6.1,6.2,6.3,6.4), and surface elevation contour map (Figure 6.6.), zone A in ERT(T1) (Figure 6.7.) is beneath the stream. As a result, the low resistivity value is attributed to the water seepage. Zones B and C are attributed to moist rock. The aerial photograph indicates that zone D and E are located in the north of sinkhole and the low resistivity values are attributed to a fractured rock with clay infilled. The low resistivity values in zone F, G, and H were attributed to the water seepage because they located beneath the natural drainage pathway.

ERT T2 (Figure 6.8.) indicated that there are seven anomalous zones in the subsurface labeled A, B, C, D, E, F, and G. As can be observed in the aerial photographs (Figure 6.1,6.2,6.3,6.4),), and surface elevation contour map (Figure 6.6.) zone A and B in ERT (T2) (Figure 6.7.) is beneath the stream. As a result, the low resistivity value is attributed to the water seepage. The aerial photograph indicates that zone C is located

beneath road; hence the low resistivity value is attributed to the seepage of the water from the ditch. Zone D and E are located in the north of sinkhole and the low resistivity values are attributed to a fractured rock filled with clay. The low resistivity values in zone F are attributed to water seepage because it located beneath the hedgerow.

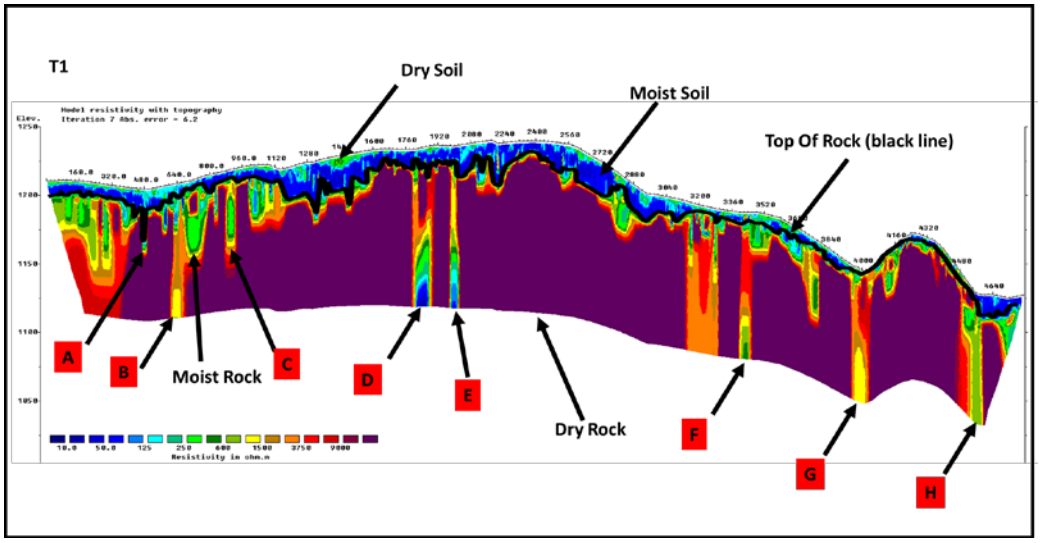

Figure 6.7. Interpreted W-E turned T1 profile in the site. Elevations and distances are in feet.

ERT T3 (Figure 6.9.) indicated that there are seven anomalous zones In the subsurface labeled A, B, C, D, E, F, and G. As can be observed in the aerial photograph (Figure 6.1, 6.2, 6.3, and 6.4),), and surface elevation contour map (Figure 6.6.) zone A in ERT (T3) (Figure 6.8.) is beneath the stream. As a result, the low resistivity value attributed to the water seepage. The aerial photograph indicates that zone D is located beneath road; hence the low resistivity value attributed to the seepage of the water from the ditch. Zone E is located in the south of sinkhole and the low resistivity values attributed to a fractured rock filled with clay. In the zone F the low resistivity

value .The low resistivity value attributed to north south trending joint set. In Zone G the low resistivity value attributed to water seepage because it located beneath the hedgerow.

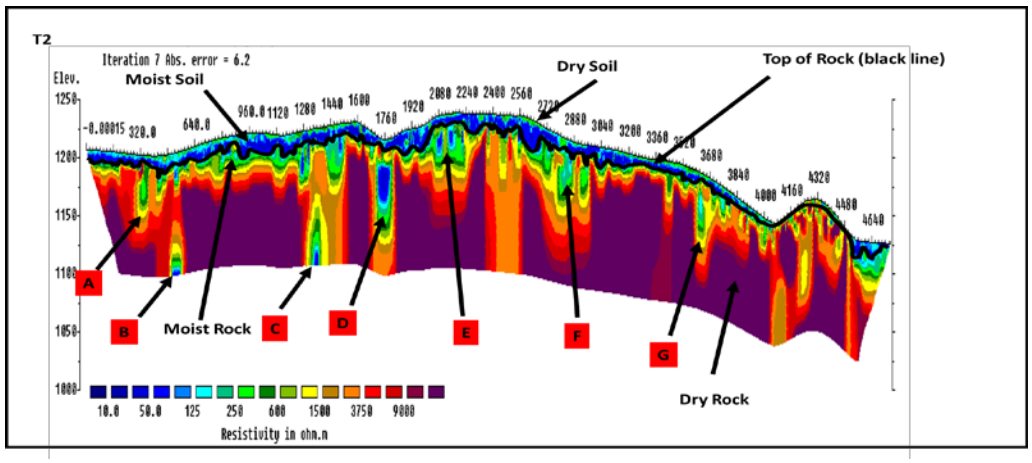

Figure 6.8. Interpreted W-E turned T2 profile in the site. Elevations and distances are in feet.

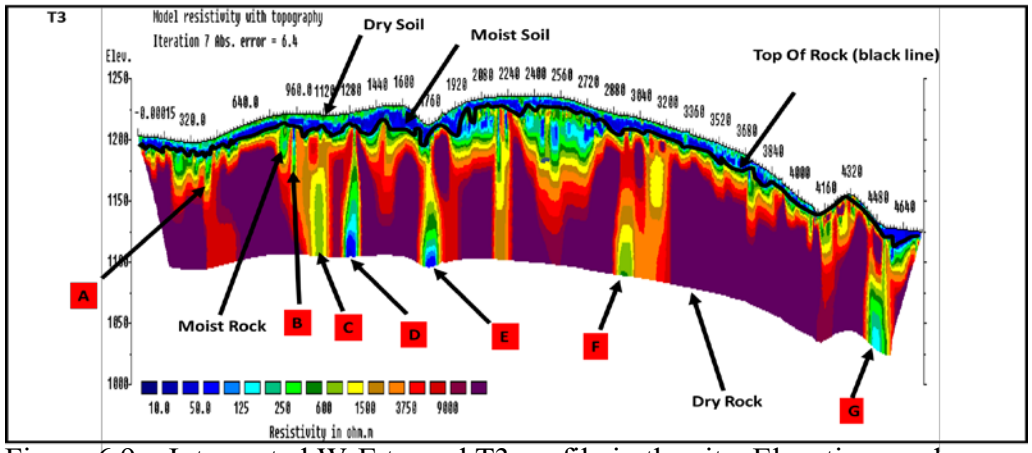

Figure 6.9. . Interpreted W-E turned T3 profile in the site. Elevations and distances are in feet.

ERT T4 (Figure 6.10.) indicated that there are seven anomalous zones In the subsurface labeled A, B, C, D, E, F, and H. As can be observed in the aerial photographs (Figure 6.1,6.2,6.3,6.4),), and surface elevation contour map (Figure 6.6.)

zone A in ERT (T4) (Figure 6.9.) is beneath the stream. As a result, the low resistivity value is attributed to the water seepage. In zone C the low resistivity value is attributed to north south trending joint set. The aerial photograph indicates that the low resistivity values in zone D is attributed to water seepage because it located beneath the hedgerow.

ERT T5 (Figure 6.11.) indicated that there are five anomalous zones

In the subsurface labeled A, B, C, D, and E. As can be observed in the aerial photographs (Figure 6.1, 6.2, 6.3, 6.4),), and surface elevation contour map (Figure 6.6.) Zone A in ERT (T5) (Figure 6.10.) is beneath the stream. As a result, the low resistivity value is attributed to the water seepage. The aerial photograph indicates that Zone B is located beneath road; hence the low resistivity value is attributed to the seepage of the water from the ditch. In Zone C the low resistivity value is attributed to north south trending joint set. In Zones D and E the low resistivity values are attributed to the seepage of the water.

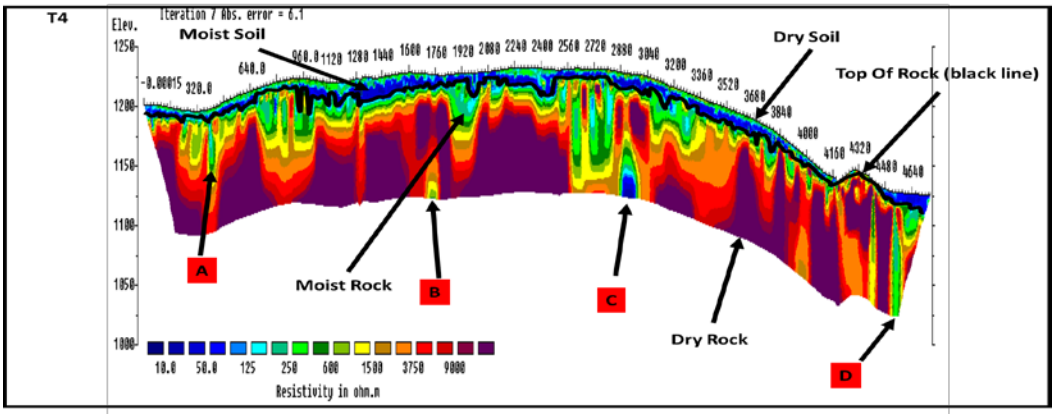

Figure 6.10. Interpreted W-E turned T4 profile in the site. Elevations and distances are in feet.

ERT T6 (Figure 6.12.) indicated that there are four anomalous zones

In the subsurface labeled A, B, C, and D. As can be observed in the aerial photographs

.

(Figure 6.1, 6.2, 6.3, 6.4), and surface elevation contour map (Figure 6.6.), zone A in ERT (T6) (Figure 6.11.) is beneath the stream. As a result, the low resistivity value is attributed to the water seepage. The aerial photograph indicates that zone B is located beneath road; hence the low resistivity value is attributed to the seepage of the water from the ditch. The zone, C is located beneath east-west hedgerow. Hence the low resistivity values are attributed to water seepage because of the hedgerow.

ERT T7 (Figure 6.13.) indicated that there are six anomalous zones

In the subsurface labeled A, B, C, D, E, and F. As can be observed in the aerial photograph (Figure 6.1, 6.2, 6.3, 6.4) and surface elevation contour map (Figure 6.6.), zone A in ERT (T7) (Figure 6.12.) is beneath the stream. As a result, the low resistivity value is attributed to the water seepage. The aerial photograph indicates that zone B is located beneath road; hence the low resistivity value is attributed to the seepage of the water from the ditch. In zone C the low resistivity value is attributed to a fractured rock with clay infilled or since it is located underneath Stray voltage (grounding) area that came from the utility column may the low resistivity value is attributed to the high conductivity. In zone D the low resistivity value is attributed to the seepage of the water. In zone E the low resistivity value is attributed to north south trending joint set. The low resistivity value in zone F is attributed to water seepage because it located beneath the hedgerow. The ERT T8 (Figure 6.14.) indicated that there are seven anomalous zones

in the subsurface labeled A, B, C, D, E, F, and G. As can be observed in the aerial photographs (Figure 6.1, 6.2, 6.3, and 6.4) and surface elevation contour map (Figure 6.6.), zone A in ERT (T8) (Figure 6.13.) is located beneath road; hence the low resistivity value is attributed to the seepage of the water from the ditch.

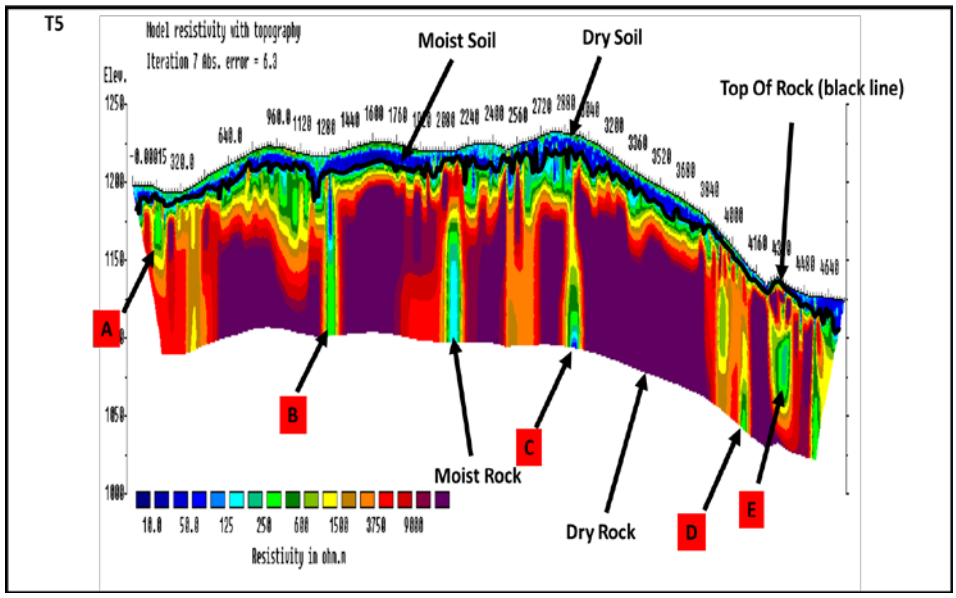

Figure 6.11. Interpreted W-E turned T5 profile in the site. Elevations and distances are in feet.

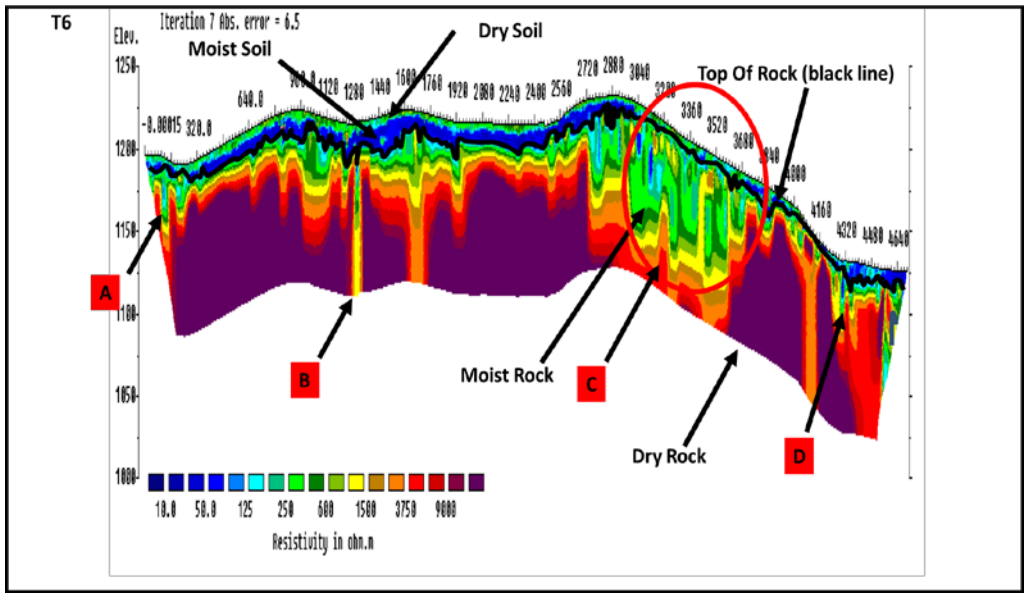

Figure 6.12. Interpreted W-E turned T6 profile in the site. Elevations and distances are in feet.

In zone B and E the low resistivity value attributed to a fractured rock with clay infilled or since it is located underneath Stray voltage (grounding) area that came from the utility column the low resistivity value may attributed to the high conductivity. In zones C and D the low resistivity values are attributed to the seepage of the water. The low resistivity values in zones F and G are attributed to water seepage because it located beneath the hedgerow.

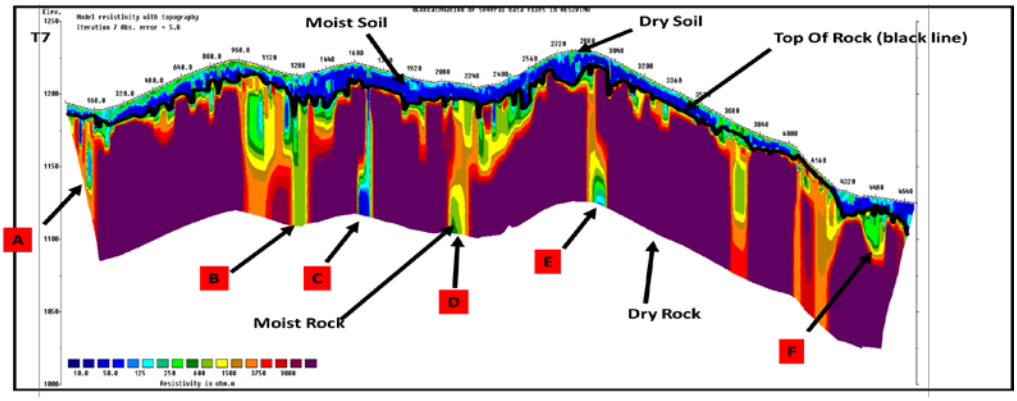

Figure 6.13.Interpreted W-E turned T7 profile in the site. Elevations and distances are in feet.

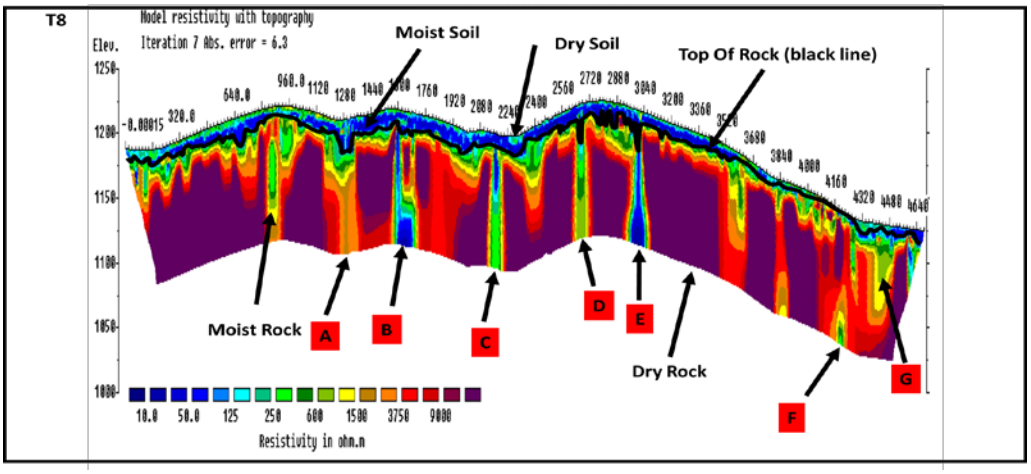

Figure 6.14.Interpreted W-E turned T8 profile in the site. Elevations and distances are in feet.

6.2. MASW DATA INTERPRETATION

The interpretations of MASW of subsurface materials were based on the shear wave velocity values. According to the National Earthquake Hazard Reduction Program (NEHRP), the standards for the rating are as following hard rock (>5000 ft/s); rock (2500 to 5000 ft/s); very dense soil and soft rock (1200 to 2500 ft/s); stiff soil (600 to 1200 ft/s) and soft soil (<600 ft/s) (Bansah et al., 2017). According to MASW 1-D shear wave velocity profiles correlated to the ERT profile T1, show that the depths to the bedrock are varied in the study area. They are approximately as shallow as 10ft. As deep as 25 ft. This is in good agreement with results found between ERT and MASW data in M1.

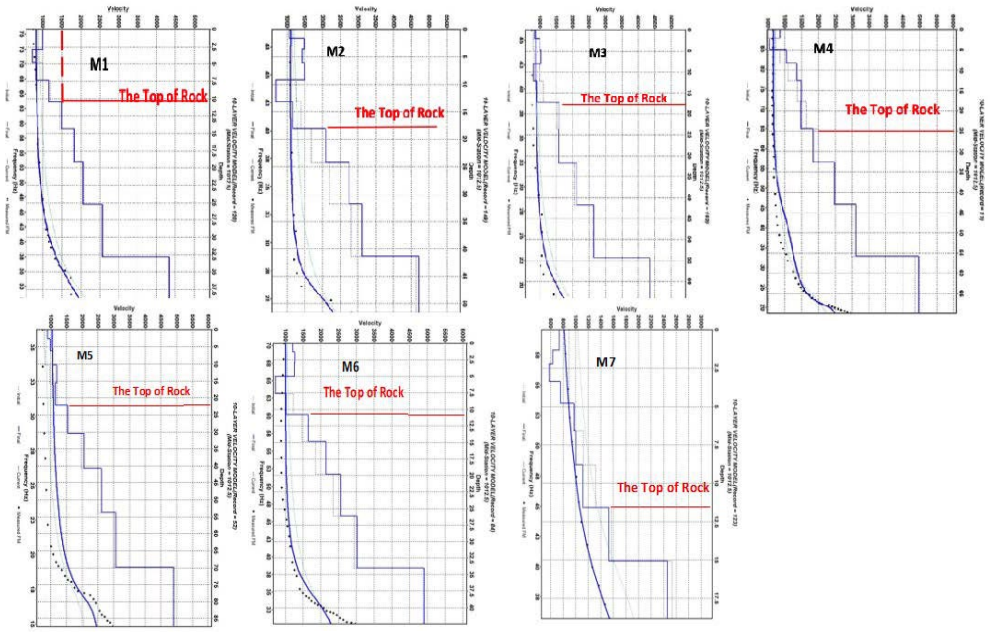

Figure 6.14. 1-D shear wave velocity profile centered on ERT (T1) profile. Interpreted depth to top of rock was 11 in M1 feet and around 12 feet on ERT profile T1.

7. CONCLUSIONS

ERT data observed in the study area show resistivity values are low in some places especially beneath the natural and anthropogenic drainage pathways due to the increased moisture content caused by infiltration of the groundwater through the fractured rocks. It was also determined that low resistivity values found in the ERT data that are not correlated to the drainage systems found in the aerial imagery of the study area can be attributed to prominent joint sets and fractured rocks filled of clay.

The subsurface, characterized by shallow rock that is pervasively fractured, was imaged to a depth of approximately 100 feet using ERT. ERT data indicates that the moisture content of subsurface is variable depending mostly on proximity to surface drainage pathways. Several drainage pathways beneath the surface through the soil and into the shallow rock, were also identified using ERT. ERT data indicates that resistivity of soil and rock beneath natural and man-made drainage pathways are often anomalously low in resistivity, an indication of higher moisture content.

ERT also indicates that in study area many zones of anomalously low resistivity are not related to sinkholes and solution-widened joints, but simply may caused by downward seepage of groundwater flowing along surface drainage pathways. This is confirmed by comparing the location of anomalies to surface aerial imagery. Overall, the interpreted ERT data correlated well with the data and MASW data in estimating the depth to the top-of-rock. The depths to the bedrocks are approximately as shallow as 3 feet and as deep as 40 feet with an average resistivity value of approximately 125 ohm-m.

This work showed that there are many low resistivity zones were observed in the study area and these zones of low resistivity zones reflect the variations in the moisture content. This work also demonstrated that when constrained using MASW and aerial imagery, ERT can be used to differentiate these anomalies as natural or man-made.

BIBLIOGRAPHY

Anderson, N. L., D. B. Apel, et al. (2006). Assessment of Karst Activity at Highway

Bansah, K. J., & Anderson, N. L. (2017, August). Multichannel Analysis of Surface Waves: Estimating Depth to Bedrock and Acoustic Properties in Karst Terrain. In 51st US Rock Mechanics/Geomechanics Symposium. American Rock Mechanics Association.

Bansah, K. J., & Anderson, N. L. MAPPING SUBSURFACE IN KARST TERRAIN USING 2-D ELECTRICAL RESISTIVITY TOMOGRAPHY.

Bansah, K., & Anderson, N. (2017, March). Factors Contributing to Karst Development in Southwestern Missouri, USA. In Symposium on the Application of Geophysics to Engineering and Environmental Problems 2017 (pp. 219-223). Society of Exploration Geophysicists and Environment and Engineering Geophysical Society.

Bullard, L., Thomson, K. C., & Vandike, J. E. (2001). The Springs of Greene County, Missouri. Missouri Department of Natural Resources, Geological Survey and Resource Assessment Division. Construction Sites Using the Electrical Resistivity Method (Greene and Jefferson Counties, Missouri).

COŞKUN, N. (2012). The effectiveness of electrical resistivity imaging in Engineering Geology, 65, 2002, p. 85-105. International Journal of Physical Sciences, 7(15).

Fellow LD (1970). Geology of Galloway Quadrangle Greene County Missouri, Missouri Geological Survey and Water Resources, pp 3-14.

Ford, D. C., & Williams, P. W. (2007). Karst hydrogeology and geomorphology (Vol. 576). Chichester: John Wiley & Sons.

https://streamstats.usgs.gov/ss/

Jennings, J.E. 1966. Building on dolomite in the Transvaal. The Civil Engineer in South Africa, 8, 42-62.

Kochanov, W.E., "Sinkholes in Pennsylvania," In www.dcnr.state.pa.us/topogeo. 1999.

Loke, M. H (2011), "Electrical Imaging Surveys for Environmental and Engineering Studies,"(http://moho.ess.ucla.edu/~pdavis/ess135_2013/literature/%20%Lokedcresistivity.pdf).

Mary McCracken, 1971, "Structural Features of Missouri," pp 5, 22-64.

Muchaidze, I. (2008). Imaging in karst terrain using electrical resistivity tomography.

Neil L. Anderson, Derek B. Apel and Ahmed Ismail, 2006, "Assessment of Karst Activity at Highway Construction Sites Using the Electrical Resistivity Method,"unpublished report for MoDOT.

Obi, J. C. (2016). Geophysical Imaging of Karst Features in Missouri. sinkhole Investigations.

T. Kidanu, S., V. Torgashov, E., V. Varnavina, A., & L. Anderson, N. (2016). ERT-based Investigation of a Sinkhole in Greene County, Missouri. AIMS Geosciences, 2(1), 99–115. https://doi.org/10.3934/geosci.2015.1.99

Vandike JE (1993) Groundwater level data for Missouri: Water year 1991-1992. Missouri Department of Natural Resources. Division of Geology and Land Survey. Water Resource Report No.42. Rolla, Missouri.

Veni, G., DuChene, H., Crawford, N. C., Groves, C. G., Huppert, G. N., Kastning, E. H., ... & Wheeler, B. J. (2001). Living with Karst: A Fragile Foundation: AGI Environmental Awareness Series 4. American Geological Institute, Alexandria, VA.

Waite, L. A., & Thomson, K. C. (1993). Development, description, and application of a geographic information system data base for water resources in karst terrane in Greene County, Missouri. Water-Resources Investigations Report ; 93-4154;, vi, 31. White, W.B. 2002. Karst Hydrology: recent development and open questions.

White, W.B. 2002. Karst Hydrology: recent development and open questions. Engineering Geology, 65, 2002, p. 85-105.

VITA

Ibrahim Alshareef was born in Makkah, Saudi Arabia on April 26, 1987. In December 2013, he received his BSc. in Geophysics from King Abdul-Aziz University Jeddah, Saudi Arabia. Right after that he started working in SGS. In July 2019, he received his M.S. in Geological Engineering from Missouri University of Science and Technology.